Functional Evolution of Clustered Aquaporin Genes Reveals Insights into the Oceanic Success of Teleost Eggs

Alba Ferré [1,†], François Chauvigné [2,†], Anna Vlasova,[3] Birgitta Norberg [4], Luca Bargelloni [5], Roderic Guigó [3,6], Roderick Nigel Finn [1,7,*], and Joan Cerdà [1,*]

[1]Institute of Agrifood Research and Technology (IRTA)-Institute of Biotechnology and Biomedicine (IBB), Universitat Autònoma de Barcelona, Barcelona, Spain

[2]Institute of Marine Sciences, Spanish National Research Council (CSIC), Barcelona, Spain

[3]Centre for Genomic Regulation (CRG), The Barcelona Institute of Science and Technology, Barcelona, Spain

[4]Institute of Marine Research, Austevoll Research Station, Storebø, Norway

[5]Department of Comparative Biomedicine and Food Science (BCA), University of Padova, Legnaro, PD, Italy

[6]Universitat Pompeu Fabra (UPF), Barcelona, Spain

[7]Department of Biology, Bergen High Technology Centre, University of Bergen, Bergen, Norway

[†]These authors contributed equally to this work.

***Corresponding authors:** E-mails: joan.cerda@irta.cat; nigel.finn@uib.no.

Associate editor: Dr. Camilla Whittington

Abstract

Aquaporin-mediated oocyte hydration is considered important for the evolution of pelagic eggs and the radiative success of marine teleosts. However, the molecular regulatory mechanisms controlling this vital process are not fully understood. Here, we analyzed >400 piscine genomes to uncover a previously unknown teleost-specific aquaporin-1 cluster (TSA1C) comprised of tandemly arranged *aqp1aa-aqp1ab2-aqp1ab1* genes. Functional evolutionary analysis of the TSA1C reveals a ∼300-million-year history of downstream *aqp1ab*-type gene loss, neofunctionalization, and subfunctionalization, but with marine species that spawn highly hydrated pelagic eggs almost exclusively retaining at least one of the downstream paralogs. Unexpectedly, one-third of the modern marine euacanthomorph teleosts selectively retain both *aqp1ab*-type channels and co-evolved protein kinase-mediated phosphorylation sites in the intracellular subdomains together with teleost-specific Ywhaz-like (14-3-3ζ-like) binding proteins for co-operative membrane trafficking regulation. To understand the selective evolutionary advantages of these mechanisms, we show that a two-step regulated channel shunt avoids competitive occupancy of the same plasma membrane space in the oocyte and accelerates hydration. These data suggest that the evolution of the adaptive molecular regulatory features of the TSA1C facilitated the rise of pelagic eggs and their subsequent geodispersal in the oceanic currents.

Key words: **functional evolution, teleosts, aquaporin, trafficking, 14-3-3 proteins, oocyte hydration.**

Article

Introduction

The most dramatic evolutionary radiation in vertebrate history occurred amongst the true spiny ray-finned fishes (Euacanthomorphacea) in the late Cretaceous and early Eocene (Maissey 1996; Friedman 2010). Fossil evidence revealed that this unprecedented radiation transpired predominantly in marine environments in a fraction of the time it took for birds and mammals to achieve such diversity (Maissey 1996; Friedman 2010). The sudden appearance of the myriad of adult forms pertaining to hundreds of new families found in fossil sites around the world suggests that key traits associated with the adaptive marine radiation of euacanthomorph teleosts were also likely associated with an efficient mechanism of dispersal. In this regard, a key reproductive trait that may have independently evolved for the first time in the Triassic in marine elopomorph teleosts (the ancestors of extant eels, bonefishes, and tarpons) was the pelagic egg, which passively drifts in the oceanic currents (Finn and Kristoffersen 2007). Upon fertilization, these free-floating, single-celled orbs of life become the caretakers of the genome, which holds the past, present, and future of the lineage. However, they are devoid of any of the organ systems or avoidance behaviors that develop in juveniles and adults, yet must equally survive in the hyperosmotic oceanic environment to ensure its continuance. Despite the lack of parental care, the selective success of this reproductive trait certainly became manifest in the euacanthomorph marine teleosts, the majority of which regardless of their systematic affinities, demersal or pelagic habitats, coastal or oceanic distribution, or tropical or boreal ranges, spawn pelagic eggs (Ahlstrom and Moser 1981; Kendall et al. 1984). Understanding the molecular adaptations

associated with the evolution of such traits could therefore shed light on how teleosts came to dominate the oceans.

The pelagic nature of marine teleost eggs is considered to have arisen as an exaptation to the recolonization of seawater (SW) by freshwater (FW) ancestors (Fyhn et al. 1999; Finn et al. 2000; Finn and Kristoffersen 2007). In this regard, it has been shown that the oocytes of oviparous marine teleosts that freely broadcast their eggs at spawning undergo substantial hydration during the phase of meiotic maturation (Finn and Fyhn 2010; Cerdà et al. 2017). Since the yolk osmolality is the same as the body fluids of the adults and thus strongly hyposmotic to SW, the hydration provides the embryos with a vital pool of water until osmoregulatory cells and organs develop (Finn et al., 2002a). The level of oocyte hydration is related to the degree of proteolysis of vitellogenin-derived yolk proteins and is most pronounced in pelagic eggs, typically resulting in water contents of >90% of the egg mass, thus reducing the specific gravity below that of the ambient SW and causing them to float (Finn 2007; Sullivan and Yilmaz 2018).

A facilitated pathway for water entry into the oocyte was discovered almost two decades ago as a teleost-specific, water-selective aquaporin (Aqp1o—now termed Aqp1ab) (Fabra et al. 2005). This channel is temporally inserted into the oocyte plasma membrane (PM) during meiotic maturation and maximal yolk proteolysis, and it is thus essential for the development of the pelagic egg phenotype (Fabra et al. 2006; Zapater et al. 2011, 2013). The Aqp1ab channel is now known to belong to a broader superfamily of aquaporins (Agre et al. 1993), which in jawed vertebrates currently comprise 17 subfamilies (Aqp0-16) (Finn et al. 2014; Chauvigné et al. 2019). Teleosts, however, retain an even larger repertoire of aquaporins, in part due to independent whole genome duplications (WGDs), but also due to more ancestral and lineage-specific tandem duplications (Tingaud-Sequeira et al. 2008, 2010; Cerdà and Finn 2010; Finn and Cerdà 2011; Finn et al. 2014; Yilmaz et al. 2020). As a result, aquaporin gene clusters became more prevalent in the actinopterygian lineage with up to seven identified to date (i.e., *aqp1aa-1ab*; *aqp3a1-3a2*; *aqp3b1-3b2*; *aqp8aa-8ab*; *aqp8ba-8bb*; *aqp10aa-10ab*; and *aqp10ba-10bb*) compared to two in the sarcopterygian lineage (*AQP3-7* and *AQP2-5-6* type clusters) (Finn et al. 2014; Yilmaz et al. 2020). The actinopterygian *aqp1ab* gene thus evolved and neofunctionalized as a downstream tandem duplicate of the *aqp1aa* paralog, which retains a more conserved protein structure to tetrapod AQP1 (Tingaud-Sequeira et al. 2008; Zapater et al. 2011).

The *aqp1aa-1ab* binary cluster has so far been detected in all teleosts studied to date, including members of the elopomorph (e.g., eels), ostariophysan (e.g., zebrafishes, carps, and catfishes), and euteleostean lineages such as protacanthopterygians (e.g., salmons) and euacanthomorphaceans (e.g., seabreams, seabasses, cichlids, flatfishes, and pufferfishes) (Cerdà et al. 2017; Zhang et al. 2021). In two of these studies, however, a second *aqp1ab*-type gene was noted in the gilthead seabream (*Sparus aurata*) and African cichlids (Zapater et al. 2013; Finn et al. 2014). In the seabream, what appeared to be exon ghosts in the 5′-promoter region of *aqp1ab* indicated that a duplicated *aqp1ab*-type pseudogene existed in this locus (Zapater et al. 2013), while in the African cichlids, each species studied retained a tetra-exon copy of the *aqp1ab* gene in the same upstream locus (Finn et al. 2014).

To decipher whether the *aqp1ab* upstream genes in teleosts were the result of lineage-specific duplications or were inherited from a common ancestor, here we initially conducted a gene-walking experiment in the seabream. This revealed a complete tetra-exon *aqp1ab*-type gene, but when ectopìcally expressed in amphibian (*Xenopus laevis*) oocytes, the translated protein was not trafficked to the PM. Surprisingly, however, phylogenetic analyses revealed that the novel seabream *aqp1ab-type* coding sequence (CDS) was more closely related to the African cichlid upstream *aqp1ab* CDS, as well as the previously studied Atlantic halibut (*Hippoglossus hippoglossus*) *aqp1ab* CDS, which was only functional in native or teleost oocytes, but not when expressed in frog oocytes (Zapater et al. 2011). These observations suggested that the upstream *aqp1ab*-type gene was likely derived from a common ancestral duplication, and that a trafficking factor present in teleost oocytes was missing in amphibian oocytes. We, therefore, conducted a systematic phylogenetic survey amongst >400 piscine genomes to uncover the ancient origin of a hitherto unknown teleost-specific *aqp1* cluster (TSA1C), comprised of *aqp1aa* and two *aqp1ab*-type genes. To understand the functional evolution of the channels in the TSA1C, we selected distantly related teleosts as models that retain one or both of the downstream *aqp1ab*-type genes. Using comparative transcriptomics and functional experiments, we reveal how the intracellular subdomains of the TSA1C channels co-evolved with teleost-specific Ywhaz-like regulatory proteins (tyrosine 3-monooxygenase/tryptophan 5-monooxygenase activation proteins or 14-3-3ζ-like) together with protein kinase-mediated phosphorylation pathways to differentially regulate their membrane trafficking. The findings provide new insight into the molecular adaptations facilitating the success of teleost eggs in the oceans.

Results

Phylogenomics Uncovers an Ancient *aqp1*-type Cluster in Teleosts

An initial gene-walking experiment using gilthead seabream genomic DNA uncovered four aquaporin-like exons 219 nucleotides (nt) upstream of the previously identified *aqp1ab* channel, and 8,144 nt downstream of the encoded *aqp1aa* gene (Fabra et al. 2005, 2006) (fig. 1A). The deduced primary structure and initial phylogenetic analysis in relation to 263 *aqp1*-type piscine CDS assembled from 94 genomes and 42 transcriptomes revealed that an additional *aqp1ab*-type channel exists in this locus (fig. 1B

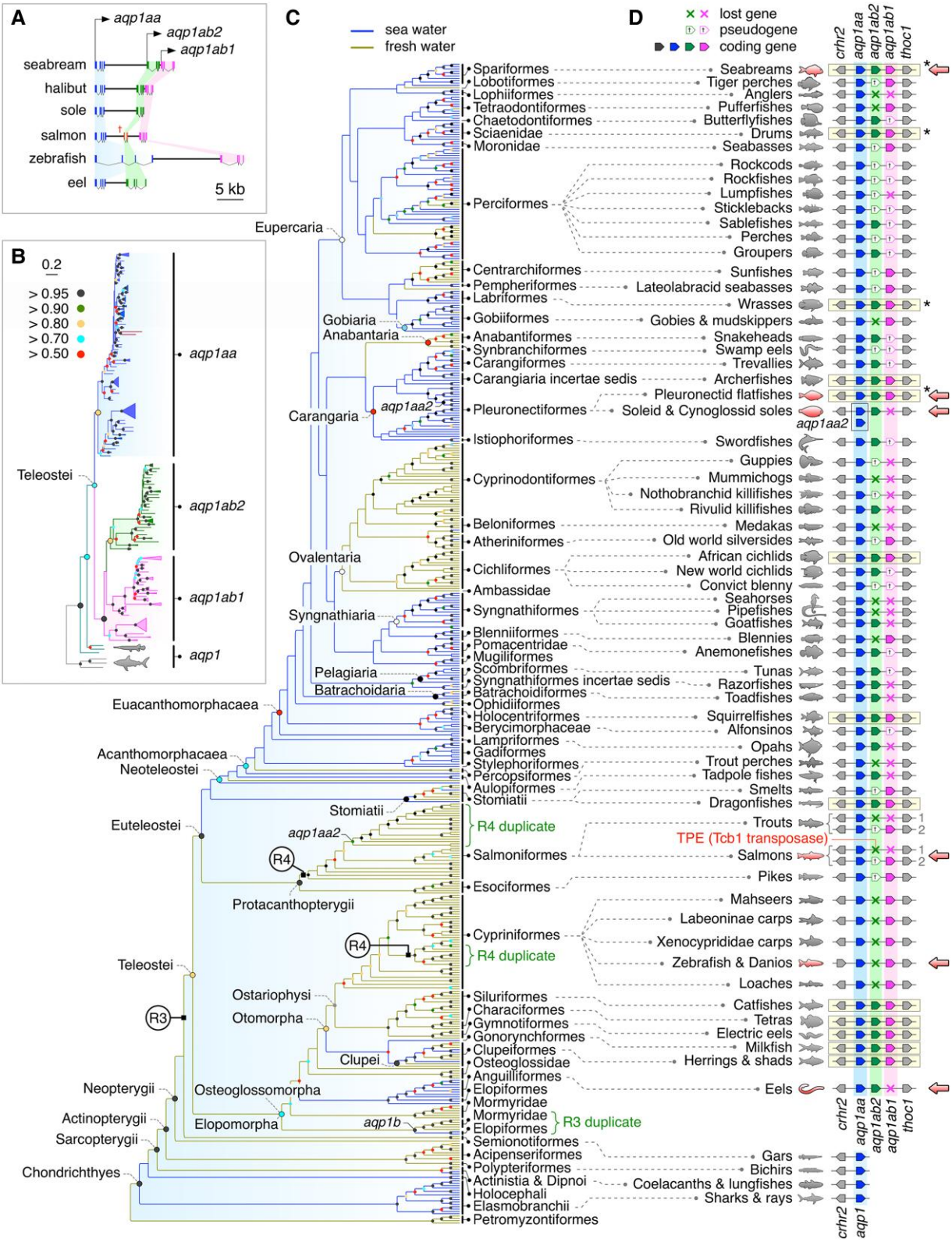

Fig. 1. The origin of the TSA1C. (*A*) Genomic organization of the TSA1C in distantly related teleosts drawn to scale. Canonical *aqp1aa*, *-1ab2*, and *-1ab1* genes consist of four exons (blue, green, and magenta bars, respectively), while pseudogenes vary from premature stop codons to highly degraded fragments (e.g., salmon†). In cypriniform teleosts (e.g., zebrafish) *aqp1ab2* is absent, while in anguilliform teleosts (e.g., eel) *aqp1ab1* is absent. (*B*) Bayesian majority rule consensus tree of the TSA1C coding sequences rooted with chondrichthyan *aqp1*. The tree is inferred from 20 million Markov Chain Monte–Carlo (MCMC) generations (nucmodel = 4by4, nst = 2, rates = gamma) of 239,282 aligned nucleotide sites aligned by codon. Support values shown at each node (colored dots) are Bayesian posterior probability ranges shown in the key. The scale bar indicates the expected rate of substitutions per site. (*C*) Bayesian majority rule consensus tree of piscine *aqp1* orthologs rooted with hyperoartian *aqp01*. The tree is initially inferred from 100 million MCMC generations (nucmodel = 4by4, nst = 2, rates = gamma) of 399,429 aligned

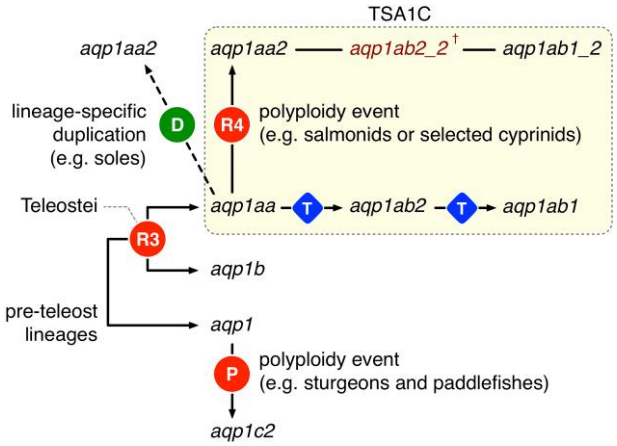

Fig. 2. The origins of multiple aquaporin-1 orthologs in fishes. Whole genome duplication (polyploidy) events (R3, R4, and P), respectively, generated *aqp1b* ohnologs in teleosts, a paralogous TSA1C in paleotetraploid salmonids and allotetraploid cyprinids and *aqp1c2* in chondrostean sturgeons and paddlefishes. Tandem duplication (*T*) gave rise to the teleost *aqp1ab2* and *aqp1ab1* paralogs. Conversely, lineage-specific duplication (*D*) generated the *aqp1aa2* paralogs in soleid and cynoglossid flatfishes.

and supplementary fig. S1, Supplementary Material online). Bayesian inference indicated that nonteleost species such as cartilaginous, chondrostean, and holostean fishes encode a single *aqp1* channel, while all teleosts have at least one *aqp1aa* gene, and different species have one or two copies of *aqp1ab* genes, which cocluster on a separate branch to the *aqp1aa* genes. In line with the convention of aquaporin nomenclature, which names genes in accordance with the chronology of their discovery, we named the second seabream *aqp1ab*-type channel and its orthologs in other species *aqp1ab2*, and renamed the original seabream *aqp1ab* channel (Fabra et al. 2005, 2006) and its orthologs in other species *aqp1ab1*. These analyses thus uncover a novel ternary TSA1C comprised of *aqp1aa-aqp1ab2-aqp1ab1*, in which the *aqp1ab2* and *aqp1ab1* genes, when present in teleost genomes, are closely juxtaposed downstream of the *aqp1aa* gene (fig. 1*A*).

The above analyses also revealed that some species of teleost harbor a second type of *aqp1aa* gene, including soleid and cynoglossid flatfishes, salmonids, and some cyprinids. In each case, however, the second *aqp1aa* gene, which we term *aqp1aa2*, coclusters within these specific lineages, and can thus be explained based on lineage-specific duplication. Thus *aqp1aa2* in salmonids is consistent with a fourth round (R4) of autotetraploidization, while that of selected cyprinids is consistent with an independent R4 allotetraploidization event (Berthelot et al. 2014; MacQueen and Johnston 2014; Xu et al. 2019). Conversely, the *aqp1aa2* gene in soleid and cynoglossid flatfishes is not found in the genomes of all other families ($n = 7$) of flatfish searched but evolved in the absence of the *aqp1ab1* gene, which is present in the genomes of pleuronectid, paralichthyid, scophthalmid, and bothid flatfishes (fig. 1*A* and *B* and supplementary fig. S1, Supplementary Material online). In tongue sole (*Cynoglossus semilaevis*), *aqp1aa2* is located on chromosome 15 (GenLoc 271 kb) and is not syntenic to the extant *aqp1aa-aqp1ab2* cluster, which is located on chromosome 20 (GenLoc 8,758 kb). From this, we surmise that the *aqp1aa2* gene of soleid and cynoglossid flatfishes is not an integral member of the TSA1C in these lineages.

Interestingly, the initial phylogenetic analysis (fig. 1*B*) indicated that the absence of the *aqp1ab1* gene is not restricted to certain families of flatfishes, but it is also absent from the genomes of other species, such as elopomorph eels, rivulid killifishes, and perciform sticklebacks, or exists as a pseudogene in scombrid tunas and perciform rockfishes (supplementary fig. S1, Supplementary Material online). Conversely, *aqp1ab2* is absent from the genomes of cyprinid fishes, including zebrafish (*Danio rerio*), gobiid mudskippers, and tetraodontiform pufferfishes, or exists as a pseudogene in the genomes of some pleuronectid, labrid, moronid, and perciform teleosts (supplementary fig. S1, Supplementary Material online). However, intact *aqp1ab2* and *aqp1ab1* genes are found in the genomes of clupeid, characiform, siluriform, cichliform, and pleuronectiform teleosts, suggesting that the TSA1C could have arisen in the common ancestor of all clupeocephalan teleosts (Otomorpha and Euteleosteomorpha). Since recent studies have revealed that aquaporin tandem duplicates of *aqp3*, *aqp8*, and *aqp10* evolved in preteleostean lineages (Cerdà and Finn 2010; Finn et al. 2014; Yilmaz et al. 2020), we conducted a separate phylogenetic analysis of *aqp1*-type genes and their syntenic loci assembled from the genomes of nonteleost fishes in relation to those of the elopomorph, osteoglossomorph, and clupeid teleosts.

The results confirmed that lampreys retain a single fused ortholog (*aqp01*) (Finn et al. 2014), while cartilaginous, sarcopterygian, and actinopterygian cladistian and holostean fishes retain a single *aqp1*-type ortholog (supplementary fig. S3, Supplementary Material online). However, two orthologs were detected in the chondrostean sturgeons and paddlefishes, and four orthologs including one or two pseudogenes were identified in osteoglossomorph teleosts such as the Aba (*Gymnarchus*

nucleotide sites aligned by codon (N = 494 taxa), with the Acanthomorphata segment of the tree re-inferred from a further 100 million MCMC generations (nucmodel = 4by4, nst = 2, rates = gamma) of 235,624 aligned nucleotide sites aligned by codon (N = 301 taxa). Whole genome duplication events (R3, R4) are indicated at relevant nodes. Support values and scale bar as in (*B*). (*D*) Syntenic arrangement of the TSA1C in selected fishes illustrating full (yellow backgrounds), partial (presence of pseudogenes), or no conservation of the cluster (both *aqp1ab*-type paralogs lost). Gene coding direction is indicated by the pointed end of each symbol with pseudogenes indicated by a white X on the symbol. Lost genes are indicated with an X. Both paralogons are shown for paleotetraploid salmonids. Asterisks indicate that some species within the group have *aqp1ab*-type pseudogenes. Red arrows highlight species selected for experimental studies. TPE: transposable element.

niloticus) or mormyrid elephantfishes (Mormyridae). Conversely, three intact orthologs were identified in elopomorph and clupeid teleosts. The phylogenetic topology of the chondrostean duplicates shows that they form a binary cluster (posterior probability [pp] = 1.0) on a sister branch to the single cladistian orthologs (pp = 1.0; supplementary fig. S3*A*, Supplementary Material online), and are located on separate chromosomes (supplementary fig. S3*B*, Supplementary Material online). This is consistent with the expected taxonomic position of Chondrostei, and an independent paleopolyploidy events in the lineage (Crow et al. 2012; Du et al. 2020). We, therefore, concluded that the chondrostean paralogs are not associated with the TSA1C, and named them *aqp1c1* and *aqp1c2*.

The phylogenetic topology of the teleost orthologs also reveals that one of the CDS assembled from the elopomorph and osteoglossomorph genomes clusters on a sister branch to the *aqp1aa* paralogs (pp = 0.8; supplementary fig. S3*A*, Supplementary Material online), yet each gene is located on a separate linkage group to the *aqp1aa-aqp1ab2-aqp1ab1* paralogs, which are all tandemly arranged in the TSA1C (supplementary fig. S3*B*, Supplementary Material online). Based upon the semiconserved synteny, we concluded that this novel *aqp1*-type ortholog found in elopomorph and osteoglossomorph teleosts represents the previously undetected ohnolog (i.e., originating from R3, the teleost-specific WGD, Amores et al. 2011; Gasanov et al. 2021), and we, therefore, named it *aqp1b*. This ohnolog was not found in any of the clupeocephalan genomes searched ($n = 365$), suggesting that it is probably lost in the vast majority (93%) of extant teleost families.

The above analyses revealed that the genomes of elopomorph teleosts such as bonefishes, tarpons, and deep-sea eels retain the *aqp1b* ohnolog together with a binary cluster of *aqp1aa-aqp1ab2* paralogs. However, although catadromous anguillimorph eels also retain the *aqp1aa-aqp1ab2* cluster, the *aqp1b* ohnolog was not found in their genomes and all elopomorph teleosts have seemingly lost the downstream *aqp1ab1* tandem duplicate. Interestingly, identification of a Tcb1-type transposase in the putative *aqp1ab1* locus suggests that gene deactivation and loss may have been associated with paleotransposon activity. Conversely, with the exception of the Aba, which appears to have a complete form of *aqp1ab2*, the genomes of most osteoglossomorph teleosts still encode intact *aqp1b* and *aqp1aa* ohnologs, but have fragmented pseudogenes of the *aqp1ab2* and *aqp1ab1* tandem duplicates (supplementary fig. S3, Supplementary Material online). Amongst clupeid teleosts, the three extant *aqp1*-type genes are all tandemly located as a ternary cluster that forms the TSA1C, with each of the *aqp1aa*, *aqp1ab2*, and *aqp1ab1* paralogs phylogenetically clustering with the same topology and high pp as shown in figure 1*B*. The only pseudogene detected was identified as a fragmented *aqp1ab1* gene in the denticle herring (*Denticeps clupeoides*).

Taken together, the above analyses reveal that the TSA1C likely evolved at the root of the crown clade of Teleostei (fig. 2), in the near aftermath of the R3 event ~300 Ma (Amores et al. 2011). The TSA1C is thus ancient but has until now been masked due to differential gene loss in various lineages. To determine whether a retention bias of either the *aqp1ab2* or *aqp1ab1* genes occurred during teleost evolution, we conducted a systematic phylogenetic analysis of the *aqp1*-type genes (fig. 1*C*, and supplementary fig. S2 and S4, Supplementary Material online) and their syntenic loci (fig. 1*D*) assembled from >400 piscine genomes. Bayesian inference of the *aqp1aa*, *aqp1b*, and nonteleost *aqp1* CDS, recovered the major groupings of piscine diversity, including the majority (85%) of teleost orders (Hughes et al. 2018), and confirmed the asymmetric retention of the *aqp1aa* gene in all teleosts, but only the *aqp1b* ohnolog in osteoglossomorph and elopomorph species. The tree further recovered the topology of the R4 duplicates in salmonids and selected cyprinids and the *aqp1aa2* duplicates in soleid and cynoglossid flatfishes. By contrast, a high number of pseudogenes of either *aqp1ab2* ($n = 105$; supplementary fig. S4*A*, Supplementary Material online) or *aqp1ab1* ($n = 72$; supplementary fig. S4*B*, Supplementary Material online) were identified, with no evidence of either paralog in 41 species. The loss or fragmentation of *aqp1ab*-type genes is thus not related to the systematic affinities of teleosts, but appears to have occurred stochastically throughout teleost evolution either in association with paleotransposon activity in salmonids and eels, or through mutation load in other species. Nevertheless, 59 species from 16 orders of teleosts still retain both the *aqp1ab*2 and *aqp1ab1* paralogs within the TSA1C. Since the biological significance of clusters of retained genes remains unclear (Albalat and Cañestro 2016), we investigated whether *aqp1ab*-type gene retention could be related to the previously established vital function of oocyte hydration and the formation of pelagic eggs (Fabra et al. 2005, 2006; Kagawa et al., 2011; Zapater et al. 2011, 2013).

Selective Retention and Expression of *aqp1ab* Genes in Marine Pelagophil Teleosts

Data on the spawning habitat (SW or FW) and type of egg spawned, that is pelagic, benthic, or internal, were compiled for 425 species of teleosts (supplementary table S1, Supplementary Material online). Pelagic eggs were defined as eggs that float freely without external buoyancy aids such as bubble nests or egg rafts. Benthic eggs included all eggs that sink in a nonlotic environment, including those that are spawned on, or are attached to substrate, egg rafts, bubble nests, or are collected by mouth brooders. Internal eggs were defined as those that are not exposed to the external environment, including those of ovoviviparous and viviparous species, as well as species that incubate their eggs in brood pouches (e.g., seahorses and pipefishes). The compiled data set reveals that approximately half (51%) of the species spawn in SW, and half (49%) spawn in FW. However, as evident in figure 1*C*, there is a systematic bias, where the more basal lineages of the

noneuacanthomorph teleosts mostly (79%) spawn in FW, while the majority (65%) of the modern euacanthomorph teleosts spawn in SW. An intriguing observation emerges when examining the euacanthomorph species ($n = 217$) in relation to the type of egg spawned and retention of *aqp1ab*-type genes. A higher proportion (60%) of the marine species from this group spawn pelagic eggs (pelagophils) as opposed to benthic (benthophils) (26%) or internally incubated eggs (14%) (supplementary fig. S5*A*, Supplementary Material online). Conversely, a greater fraction (81%) of the FW species are benthophils as opposed to pelagophils (1%), and there is no significant difference between the proportions of species in SW (14%) or FW (18%) with internal egg development. Most striking is that nearly all of the pelagophils (95%) retain at least one of the *aqp1ab2* or the *aqp1ab1* genes, with a third of the species (33%) retaining both paralogs (supplementary fig. S5*B*, Supplementary Material online). This level of gene retention is much higher when compared to that of the benthophils (57% retain 1 paralog; 12% retain both paralogs), and greatly exceeds that of species that incubate their eggs internally, where no species retains both paralogs, and 91% no longer possess the TSA1C. Quantitative analyses of the mRNA expression levels in different adult tissues further revealed that *aqp1ab*-type transcripts are highly enriched in the ovaries of marine pelagophil species, such as pleuronectids, soleids, and sparids, but not those of FW benthophils such as salmonids and cyprinids (supplementary fig. S6, Supplementary Material online; Tingaud-Sequiera et al. 2008).

Intracellular Trafficking of the TSA1C is Differentially Regulated

To better understand the evolutionary basis of the above observations and to investigate how species that retain both *aqp1ab1* and *aqp1ab2* paralogs can avoid expression redundancy of their channel products, we functionally characterized each channel in the TSA1C from distantly related marine and FW teleosts. These species included those that retain one of the downstream *aqp1ab*-type genes, such as the elopomorph European eel (*Anguilla anguilla*), the ostariophysan zebrafish, and stinging catfish (*Heteropneustes fossilis*), the protacanthopterygian Atlantic salmon (*Salmo salar*) and the euacanthomorph Senegalese sole (*Solea senegalensis*), and two euacanthomorph marine teleosts that retain both *aqp1ab*-type genes, the Atlantic halibut and the gilthead seabream. These species also spawn different types of eggs with zebrafish, salmon, and catfish producing benthic eggs, while sole, seabream, and halibut produce highly hydrated pelagic eggs.

To determine whether the TSA1C paralogs from each model species encode functional water channels, we used oocytes from *X. laevis* as standard surrogate experimental systems for the fish oocytes (Chauvigné et al. 2021). Oocytes were injected with the corresponding cRNAs, synthesized from nontagged or human influenza hemagglutinin (HA)-tagged cDNAs, or with water as negative controls, and subsequently submitted to swelling assays (fig. 3). Oocytes expressing Aqp1aa from zebrafish (DrAqp1aa), European eel (AaAqp1aa), Atlantic salmon (SsaAqp1aa), gilthead seabream (SaAqp1aa), Atlantic halibut (HhAqp1aa), or Senegalese sole (SseAqp1aa) showed a 6–11-fold increase in osmotic water permeability (P_f) with respect to the control oocytes after a hypoosmotic challenge, whereas oocytes injected with SseAqp1aa2 showed a P_f increment of ∼3 times (fig. 3*A*). However, with respect to the controls, oocytes expressing DrAqp1ab1, SsAqp1ab1, SaAqp1ab1, or HhAqp1ab1 only showed ∼4-fold increase in P_f, while those expressing AaAqp1ab2, SaAqp1ab2, HhAqp1ab2, SseAqp1ab2, or Aqp1ab2 from the stinging catfish (HfAqp1ab2), displayed even less swelling with ∼1-fold increase in P_f (fig. 3*B* and *C* and supplementary fig. S7*A* and *B*, Supplementary Material online).

To investigate the intracellular trafficking to the *X. laevis* oocyte PM of the TSAC1channels, we employed immunoblotting and immunofluorescence microscopy using paralog-specific or anti-HA antibodies. These experiments revealed that teleost Aqp1aa polypeptides were constitutively expressed at the PM (fig. 3*D*). In contrast, the Aqp1ab1 and -1ab2 channels were differentially retained in the cytoplasm (fig. 3*E* and *F*), thus explaining the lower P_f of oocytes expressing these paralogs compared to those injected with Aqp1aa. Double immunostaining of Aqp1ab1 or -1ab2 with the endoplasmic reticulum (ER) marker protein disulfide isomerase (PDI) further revealed that both channels colocalized with the PDI (fig. 3*G* and *H* and supplementary fig. S7*C* and *D*, Supplementary Material online), suggesting an impaired sorting of these aquaporins from the ER to the frog oocyte PM. Transient expression of flag-tagged Aqp1aa, -1ab1, or -1ab2 from different teleosts in the human breast cancer cell line Michigan Cancer Foundation-7 confirmed the constitutive expression of teleost Aqp1aa in the PM, as well as the differential retention of Aqp1ab1 and -1ab2 in the ER (supplementary fig. S8*A*–*C*, Supplementary Material online). However, these trials also showed a stronger colocalization of Aqp1ab2 with the lysosomal-associated membrane protein 1 compared to that of Aqp1ab1 (supplementary fig. S8*D* and *E*, Supplementary Material online), indicating that the Aqp1ab2 channels are also rapidly redirected to lysosomal degradation.

Protein Kinases Regulate the Intracellular Trafficking of the TSA1C Channels

Since intracellular trafficking of aquaporins is often regulated by protein kinase-mediated phosphorylation of subdomain-specific residues (Nesverova and Törnroth-Horsefield 2019), we initially tested whether protein kinase A (PKA) and C (PKC) activators, forskolin (FSK), and phorbol 12-myristate 13-acetate (PMA), respectively, could regulate the trafficking of Aqp1aa, -1ab1, or -1ab2 from each model teleost species in *X. laevis* oocytes (supplementary fig. S9, Supplementary Material online). Subsequently, to identify the potential amino acid residues involved, we conducted in silico searches for putative PKA-

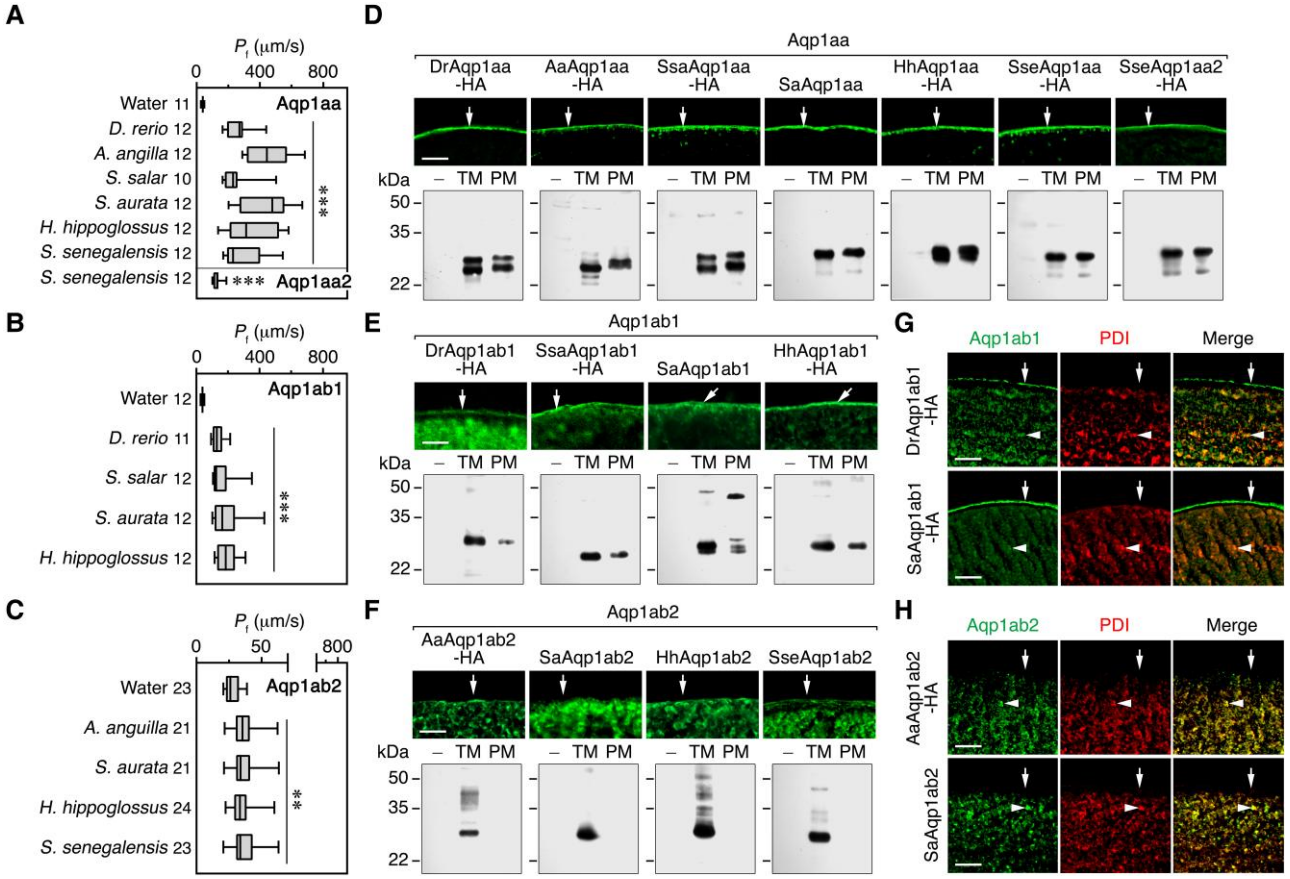

Fig. 3. Functional characterization of Aqp1-like channels in teleosts. (*A*–*C*) Osmotic water permeability (P_f) of *X. laevis* oocytes injected with water (controls) or expressing WT Aqp1aa, -1ab1, or -1ab2 paralogs from different teleosts. All data points are presented as box and whisker plots/scatter dots with horizontal line (inside box) indicating median and outliers. The number of oocytes in each group is indicated on the left of each plot. Data were statistically analyzed by an unpaired Student's *t*-test (**$P < 0.01$; ***$P < 0.001$; with respect to controls). (*D*–*F*) Immunolocalization (upper panels) and immunoblot (lower panels) of the different intact or HA-tagged channels (as indicated) in oocytes. Proteins were detected by using an anti-HA commercial antibody or paralog-specific antibodies. Molecular mass markers (kDa) are on the left. TM, total membrane; PM, plasma membrane. (*G*, *H*) Double immunostaining of oocytes expressing zebrafish or seabream Aqp1ab1, or European eel or seabream Aqp1ab2, and the ER marker PDI. The PM of oocytes is indicated by arrows (D–H), whereas the arrowheads (G and H) indicate colocalization of the channels with the PDI. Scale bars, 25 µm.

or PKC-mediated phosphorylation sites in the intracellular loop D and C-termini of the channels, followed by site-directed mutagenesis experiments (supplementary fig. S10, Supplementary Material online). The data confirmed that PKC positively regulates PM trafficking of human AQP1, as well as the Aqp1aa orthologs from elopomorph and cyprinid teleosts (AaAqp1aa and DrAqp1aa) through phosphorylation of conserved Thr residues in loop D. In contrast, in modern euteleost lineages (SaAqp1aa, SseAqp1aa, and SseAqp1aa2), this mechanism switches to negative regulation of Aqp1aa trafficking due to substitution of the upstream Thr by a Val residue. These experiments also revealed that PKA mediates positive membrane trafficking of Aqp1aa orthologs from elopomorph and cyprinid teleosts through phosphorylation of conserved C-terminal Ser residues, but not in euacanthomorph species (SaAqp1aa and SseAqp1aa2). By contrast, the trafficking of the Aqp1ab1 paralog was negatively regulated by PKC in the cyprinid and salmonid teleosts (DrAqp1ab1 and SsaAqp1ab1), which surprisingly appeared to be linked to the presence of two Thr-Thr residues in loop D, whereas that of Aqp1ab2 was stimulated by PKC but only in the elopomorph European eel (AaAqp1ab2). Activation of PKA promoted Aqp1ab1 PM trafficking in all the teleost species tested, however, the involved phosphorylation sites could not be determined using current prediction algorithms. The same positive effect of PKA on channel trafficking was only conserved in Aqp1ab2 from species that retain only this paralog, such as European eel and sole. Interestingly, we also identified p38 mitogen-activated protein kiknase (MAPK) putative phosphorylation sites conserved in the Aqp1ab1 C-termini of most (74%) of the euteleost species examined (supplementary fig. S10*F*, Supplementary Material online), which reduce PM trafficking (Tingaud-Sequeira et al. 2008). Such p38 MAPK sites are not found in the otophysan lineages of siluriform and clupeiform teleosts that also retain intact *aqp1ab1* genes. These data thus suggest that the intracellular trafficking of the TSA1C is differentially regulated by PKA and PKC, and also by p38 MAPK in the case of Aqp1ab1,

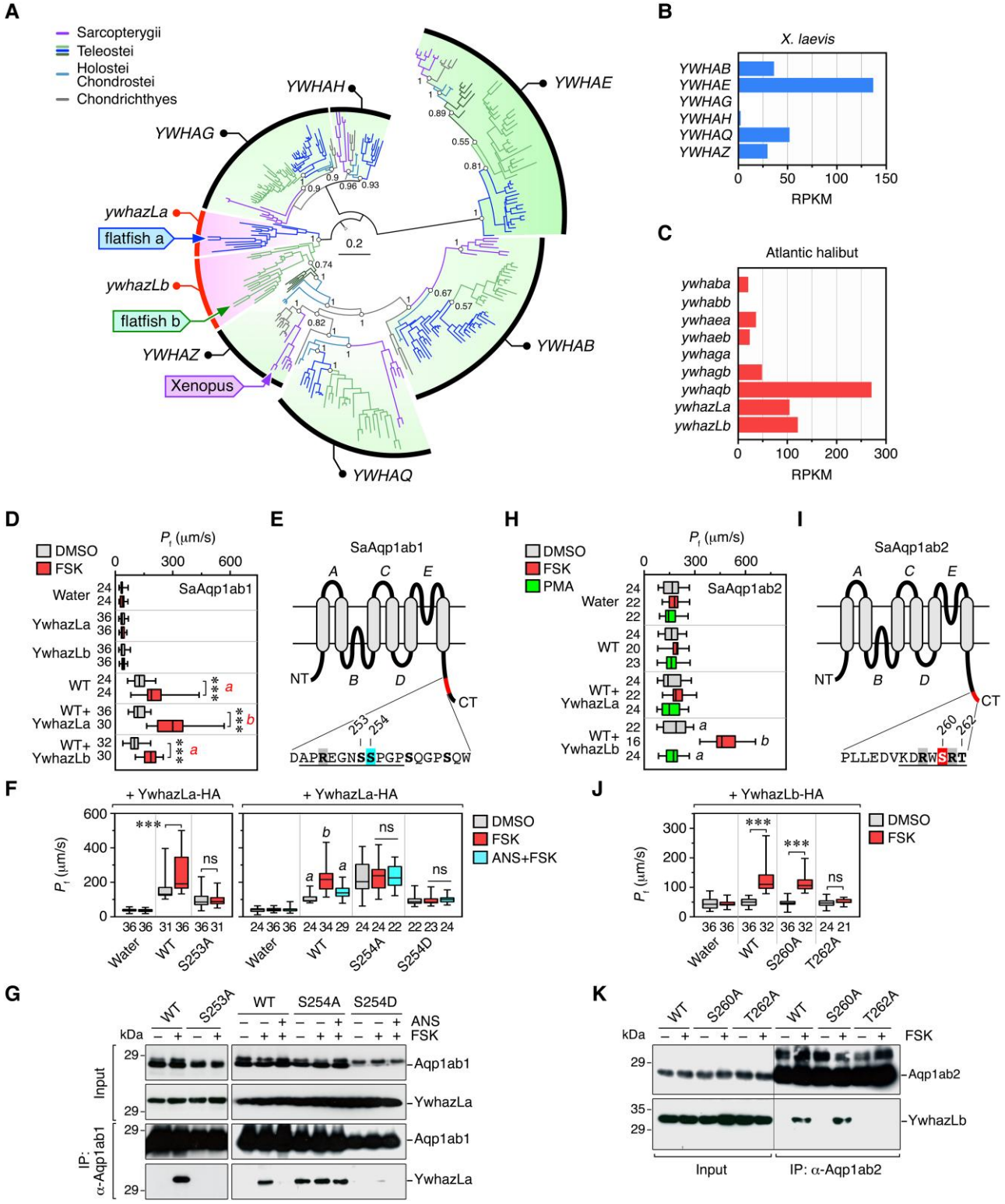

FIG. 4. Identification of teleost-specific YWHA proteins and regulation of Aqp1ab1 and -1ab2 trafficking. (*A*) Bayesian majority rule midpoint rooted consensus tree (3 million MCMC generations inferred from 278,404 nucleotide sites) from 337 gnathostomes *YWHA* coding sequences. Posterior probabilities are shown at selected nodes (see supplementary figs. S13 and S14, Supplementary Material online for fully annotated trees). *X. laevis YWHAZ* and flatfish *ywhazLa* and *-zLb* branches are respectively indicated. (*B* and *C*) Expression levels were assessed as reads per kilo base per million mapped reads (RPKM) of transcripts encoding YWHA proteins in the *X. laevis* and Atlantic halibut ovarian follicle transcriptomes. (*D*, *H*) P_f of *X. laevis* oocytes injected with water or expressing WT SaAqp1ab1 (*D*) or SaAqp1ab2 (*H*), with or without co-injection of HA-tagged seabream YwhazLa or -zLb, respectively, and treated with DMSO, FSK (PKA activator), or PMA (PKC activator). (*E*, *I*) Schematic representation of SaAqp1ab1 and -1ab2 monomers showing the six transmembrane domains, the five connecting loops (A-E), and the predicted YWHA-binding regions (underlined) in the C-termini (see also supplementary fig. S10, Supplementary Material online). Residues shaded in blue and red indicate putative PKA and p38 MAPK-phosphorylation sites, respectively. (*F*, *J*) P_f of oocytes injected with water or expressing WT

but that the specific residues involved in these regulations appear to have changed with the evolution of the different lineages.

Novel Teleost Ywhaz-Like Binding Proteins Regulate Aqp1ab1 and -1ab2 Trafficking

Although the previous experiments could not determine the specific mechanisms involved in the trafficking regulation of Aqp1ab1 and -1ab2 in some teleosts, experiments using chimeric proteins indicated that the Aqp1ab1 and -1ab2 C-termini are mechanistically associated with the cytoplasmic retention of the channels in amphibian oocytes (supplementary fig. S11, Supplementary Material online). Further *in silico* analysis of the C-termini of teleost Aqp1ab1 and -1ab2 revealed the presence of potential binding motifs for YWHA (14-3-3) regulatory proteins (supplementary fig. S10*F* and *J*, Supplementary Material online), which can bind membrane proteins in a PKA-mediated Ser/Thr phosphorylation-dependent manner to regulate their function and subcellular sorting (Fu et al. 2000; Moeller et al. 2016; Prado et al. 2019). The YWHA interaction motif in the target protein usually contains an Arg residue that increases binding affinity (Rajan et al. 2002; Shikano et al. 2005). Therefore, to investigate whether YWHA proteins could regulate teleost Aqp1ab1 and -1ab2 trafficking, as well to establish which specific residues could be involved in these mechanisms, we conducted a mutagenesis screen in which the C-terminal Arg within the predicted YWHA motif was substituted by Ala, and all potential phosphorylation sites in this subdomain were separately replaced by Asp to mimic a constitutive phosphorylation state (supplementary fig. S12, Supplementary Material online). The results of these experiments for the Aqp1ab1 channels appeared to be puzzling among species, but the data did suggest that binding of Aqp1ab2 to a teleost-specific YWHA carrier protein might be involved in the regulation of channel trafficking.

To identify teleost-specific YWHA paralogs that could facilitate Aqp1ab1 and -1ab2 membrane trafficking, we conducted a comparative transcriptomic analysis of Atlantic halibut postvitellogenic and *X. laevis* stage IV ovarian follicles by RNA sequencing (supplementary table S2, Supplementary Material online). In parallel, we further constructed a phylogenetic tree of the vertebrate YWHA-binding proteins with a view to finding teleost-specific duplicates that display long branch lengths and thus potential neofunctionalization in relation to the amphibian orthologs. Bayesian inference of the CDS of the YWHA-encoding transcripts shows that teleosts and amphibians have orthologs of the mammalian *YWHAB*, *YWHAE*, *YWHAG*, *YWHAH*, *YWHAQ*, and *YWHAZ* subfamilies (fig. 4*A*, and supplementary fig. S13, Supplementary Material online). Teleost duplicates were identified in each subfamily, except *YWHAH*, with the longest branch lengths in relation to the single *X. laevis* orthologs noted for *YWHAQ* and *YWHAZ*. The *YWHAQ* cluster recovered the expected interrelationships of Chondrichthyes, Actinopterygii, and Sarcopterygii, however, the duplicated *ywhaqa* and *ywhaqb* orthologs were restricted to noneuacanthomorph species, with only the *ywhaqb* gene found in the Euacanthomorphacea. By contrast, both of the teleost duplicates within the *YWHAZ* cluster are found in the Euacanthomorphacea but formed more distantly related clusters external to the nonteleost actinopterygian, chondrichthyan, and sarcopterygian CDS. We, therefore, named these novel teleost-specific duplicates Ywhaz-like-a (*ywhazLa*) and Ywhaz-like-b (*ywhazLb*). Using this initial analysis as a framework, we searched the halibut and *X. laevis* transcriptomes to establish which of the YWHA genes are expressed in the respective ovarian follicles. The orthology of each identified transcript was confirmed by Bayesian inference (supplementary fig. S14*A*–*E*, Supplementary Material online), and revealed that the *YWHAB*, *YWHAE*, *YWHAQ*, and *YWHAZ* paralogs are each expressed in the *X. laevis* follicle with *YWHAE* showing the highest expression (fig. 4*B*). In the halibut follicle, the *ywhaqb*, *ywhazLa*, and *ywhazLb* transcripts showed the highest expression, whereas *ywhaba*, *ywhaea*, *ywhaeb*, and *ywhagb* were expressed at relatively lower levels (fig. 4*C*).

The above results highlighted YwhazLa and -zLb as candidate binding proteins that could have duplicated and neofunctionalized to a degree that is specific to modern euacanthomorph teleosts. Thus, although *X. laevis* oocytes express orthologous YWHA proteins that can facilitate the heterologous membrane trafficking of the teleost Aqp1aa and -1ab1 paralogs, amphibian YWHA proteins may no longer possess the specificity required for trafficking the Aqp1ab2 channel. To test this hypothesis, we conducted further experiments using site-directed mutagenesis and co-immunoprecipitation to detect aquaporin-YwhazL interactions, where seabream YwhazLa and -zLb cRNAs were co-expressed with those of Aqp1ab1 and -1ab2 of distantly related teleosts in *X. laevis* oocytes. The results suggested that PM trafficking of teleost Aqp1ab1 channels (DrAqp1ab1, SsaAqp1ab1, SaAqp1ab1, and HhAqp1ab1) in response to PKA phosphorylation can be regulated by endogenous frog YWHA proteins, but that this mechanism is more efficiently controlled by the binding to

SaAqp1ab1 (*F*) or WT SaAqp1ab2 (*J*), or mutant channels at specific residues potentially involved in YwhazL binding, and treated with FSK alone or in the presence of the p38 MAPK activator ANS. Control and aquaporin expressing oocytes were also co-injected with YwhazLa-HA or -zLb-HA as above. (*G*, *K*) Co-immunoprecipitation of Aqp1ab1 and YwhazLa (*G*), or Aqp1ab2 and YwhazLb (*K*), in oocytes treated as in F and J, respectively. The IP using an anti-HA or anti-SaAqp1ab1 and -1ab2 specific antibodies (in G and K, respectively) were immunoblotted with appropriate antibodies (as indicated). Molecular mass markers (kDa) are on the left. In D, H, H, and J, data are presented as box and whisker plots with the number of oocytes in each group indicated on the left or below each plot. Data were analyzed by the unpaired Student's *t*-test (*$P < 0.05$; **$P < 0.01$; ***$P < 0.001$; as indicated in brackets). In D and H, letters indicate significant differences in one-way analysis of the variance (ANOVA) ($P < 0.05$). ns, statistically not significant.

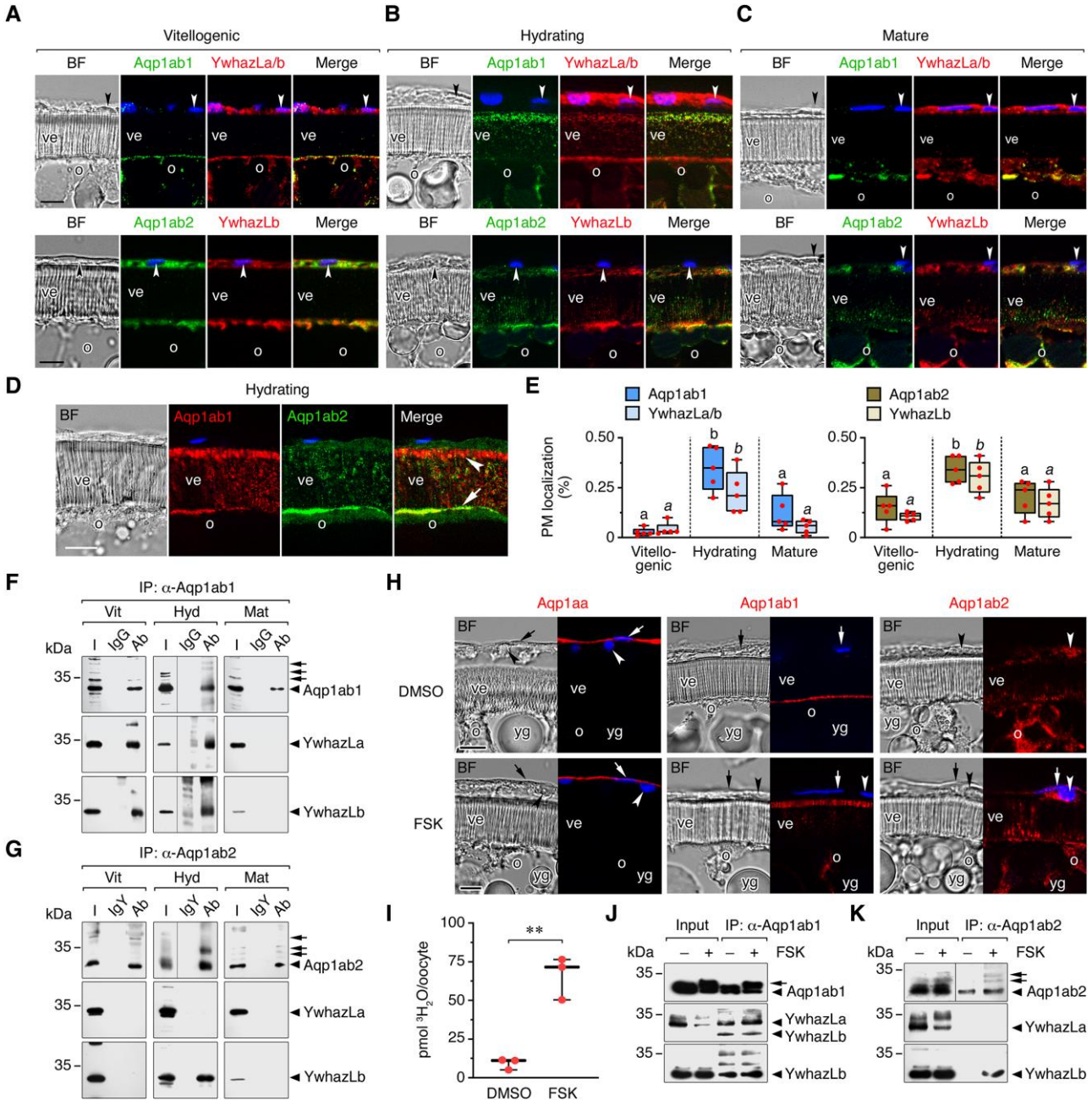

Fig. 5. Aqp1ab1 and -1ab2 PM trafficking and YwhazL interaction is regulated during seabream oocyte hydration in vivo and vitro. (*A*–*C*) Double immunostaining of Aqp1ab1 (green) and YwhazLa/b (red), and Aqp1ab2 (green) and YwhazLb (red), in ovarian follicles enclosing vitellogenic (Vit; A), hydrating (Hyd; B), or mature (Mat; C) oocytes. The granulosa (arrowheads) and theca (arrows) cells are counterstained with DAPI (blue). Abbreviations: vitelline envelope; o, oocyte; yg, yolk globule. Control sections are shown in (supplementary fig. S21*B*, Supplementary Material online). Scale bars, 10 µm. (*D*) Double immunostaining of Aqp1ab1 (red; arrowhead) and -1ab2 (green; arrow) in hydrating oocytes. Scale bars and abbreviations as in A–C. (*G*) Fluorescence quantitative estimation of the amount of Aqp1ab1, -1ab2, YwhazLa/b, and -zLb in the PM of oocytes during hydration. (*F*, *G*) Co-immunoprecipitation of Aqp1ab1 (*F*) or -1ab2 (*G*) and YwhazLa and -zLb in Vit, Hyd, and Mat follicles. The IP using seabream Aqp1ab1 and -1ab2 specific antibodies (in F and G, respectively) were immunoblotted with appropriate antibodies as indicated. Phosphorylated forms of the channels are indicated by arrows, whereas aquaporin and YwhazL monomers are indicated by arrowheads. I, input; IgG or IgY, immunoglobulin G or Y; Ab, immunoprecipitating antibody. In F-G and J-K, molecular mass markers (kDa) are on the left. (*H*) Immunostaining of Aqp1aa, -1ab1, and -1ab2 in postvitellogenic ovarian follicles treated with DMSO (control) or FSK in vitro. Labels as in A–C. Scale bar, 10 µm. (*I*) Uptake of ^3H_2O by follicle-enclosed oocytes treated with DMSO or 3-Isobutyl-1-methylxanthine (IBMX)/FSK. (*J*, *K*) Co-immunoprecipitation of Aqp1ab1 (*J*) or -1ab2 (*K*) and YwhazLa and -zLb in postvitellogenic follicles treated or not with IBMX/FSK. Labels as in F-G. Data in E and I are presented as box and whisker plots with the number of follicles (*E*) or pools of ten follicles (*I*) analyzed indicated by dots, and were analyzed by ANOVA ($P < 0.05$; different letters indicate significant differences for each protein) or an unpaired Student's *t*-test (**$P < 0.01$), respectively.

the teleost-specific YwhazLa paralogs (fig. 4D and supplementary figs. S15A–F and S17A, Supplementary Material online). In the cyprinid zebrafish, the data confirmed the presence of two PKA mechanisms regulating Aqp1ab1 trafficking, one dependent on the phosphorylation status of Ser^{261} in the C-terminus of the channel for YwhazLa binding, and another independent of YwhazLa interaction and controlled by Ser^{263} phosphorylation (supplementary figs. S12A and S15G and H, Supplementary Material online). In contrast, in the marine euacanthomorph teleost seabream (SaAqp1ab1) (fig. 4E–G), as well as in salmonids (SsaAqp1ab1) (supplementary figs. S17B, Supplementary Material online), apparently, only one mechanism based on PKA phosphorylation of C-terminal Ser^{253} and Ser^{258}, respectively, regulates the YwhazLa interaction and channel trafficking. These data indicate that although salmonids only retain the Aqp1ab1 paralog as do cyprinids, the salmonid Aqp1ab1s have lost the second YwhazLa-independent PKA regulatory mechanism for channel trafficking. We further observed that the p38 MAPK-mediated phosphorylation sites within the YWHA-binding domain in the Aqp1ab1 C-termini of salmonid and euacanthomorph teleosts (Ser^{252}-Ser^{253} and Ser^{254} in salmon and seabream, respectively) prevent the YwhazLa interaction resulting in recycling of the channel (fig. 4E–G and supplementary fig. S17B and C, Supplementary Material online).

For Aqp1ab2, we found that in the elopomorph eel trafficking of the channel is preferentially regulated by PKA-mediated YwhazLa binding, through phosphorylation of C-terminal Ser^{241} (supplementary fig. S16A, C, E, and G, Supplementary Material online), as observed for DrAqp1ab1. However, eel AaAqp1ab2 also retains a YwhazLa-independent mechanism for channel trafficking, which is mediated by dual PKC phosphorylation of Ser^{255} in the C-terminus (supplementary fig. S16G, Supplementary Material online) and of Thr^{148} in loop D (supplementary figs. S10J and K, Supplementary Material online). In contrast, in all the euacanthomorph marine teleosts investigated, Aqp1ab2 trafficking is specifically (SaAqp1ab2 and HhAqp1ab2) or partially (SseAqp1ab2) dependent on YwhazLb interaction (fig. 4H and supplementary fig. S16B, D, and F, and S17D, Supplementary Material online). Thus, in seabream, halibut, and sole, the interaction depends on PKA phosphorylation of Thr^{262}, Ser^{241}-Ser^{242}, and Ser^{242}, respectively (fig. 4I and J and supplementary fig. S17E and F, Supplementary Material online). PM targeting of SseAqp1ab2 is also regulated by PKA phosphorylation of Thr^{233} outside of the predicted YWHA interacting region, but this mechanism still depends on YwhazLa or -zLb binding, since inhibition of this interaction prevents PKA-mediated trafficking of the channel to the PM (supplementary fig. S17F, Supplementary Material online).

The Ywhaqb paralog, also highly expressed in halibut ovarian follicles, did not have any positive effect on seabream Aqp1ab1 or -1ab2 trafficking (supplementary fig. S18, Supplementary Material online). Therefore, our observations suggest that Aqp1ab-type trafficking regulation evolved from a relatively relaxed, low-specificity YWHA-binding requirement that has been maintained in species that retain only one of the channels, albeit with a slight binding preference for Aqp1ab1 to YwhazLa. However, a highly constrained binding requirement of Aqp1ab2 to YwhazLb evolved in euacanthomorph species that retain both of the Aqp1ab-type channels. In addition, the pre-euteleost Aqp1ab1 channels evolved YWHA-independent phosphorylation mechanisms for trafficking to the PM, while the euteleost channels evolved recycling mechanisms mediated by p38 MAPK-phosphorylation.

In Vivo Aqp1ab1 and -1ab2 PM Trafficking and YwhazL Binding is Regulated to Facilitate Oocyte Hydration During Meiosis Resumption

To investigate the physiological significance of YwhazL regulation of the TSA1C trafficking, we determined the in vivo dynamics of the subcellular localization of endogenous Aqp1aa, -1ab1, and -1ab2, and their interactions with YwhazLa and -zLb proteins, during teleost oocyte hydration. For this, we employed the seabream as a model organism for marine euacanthomorph teleosts (supplementary fig. S19, Supplementary Material online) and paralog-specific antisera (supplementary fig. S20A and B, Supplementary Material online).

Immunofluorescence microscopy showed that the expression of Aqp1aa was restricted to the theca cells surrounding vitellogenic ovarian follicles, and this localization did not change during oocyte hydration (supplementary fig. S21A, Supplementary Material online). In contrast, both Aqp1ab1 and -1ab2 were localized in the most cortical region of the ooplasm, while Aqp1ab2 was also detected in the granulosa and theca cells (fig. 5A). During oocyte hydration, Aqp1ab1 almost disappeared from the oocyte cortical cytoplasm and accumulated in the most distal part of the microvilli crossing the vitelline envelope, whereas Aqp1ab2 became localized in a more basal region of the microvilli (fig. 5B and D). In hydrated mature oocytes, Aqp1ab1 and -1ab2 signals were no longer observed in the microvilli or were greatly reduced, respectively (fig. 5C). Immunoblotting and double immunolocalization experiments using seabream YwhazLa/b- or -zLb specific antibodies showed the colocalization of Aqp1ab1 and YwhazLa/b signals in the oocyte, as well as of those of Aqp1ab2 and YwhazLb (fig. 5A–C), with their abundance in the PM increasing during the hydration process (fig. 5E). Concomitantly, increased phosphorylation of Aqp1ab1 and -1ab2 was only observed in follicles enclosing hydrating oocytes (supplementary fig. S19C and D, Supplementary Material online). However, co-immunoprecipitation revealed that Aqp1ab1 already interacts with YwhazLa and -zLb in vitellogenic follicles, with the interaction being maintained during oocyte hydration and terminated in mature follicles (fig. 5F), whereas Aqp1ab2 only binds to YwhazLb in follicles containing hydrating oocytes (fig. 5G).

To confirm that PKA activation triggers Aqp1ab1 and -1ab2 phosphorylation and the YwhazL interactions in oocytes, we incubated isolated seabream vitellogenic ovarian follicles in vitro in the presence or absence of FSK. These experiments showed that FSK triggered the translocation of

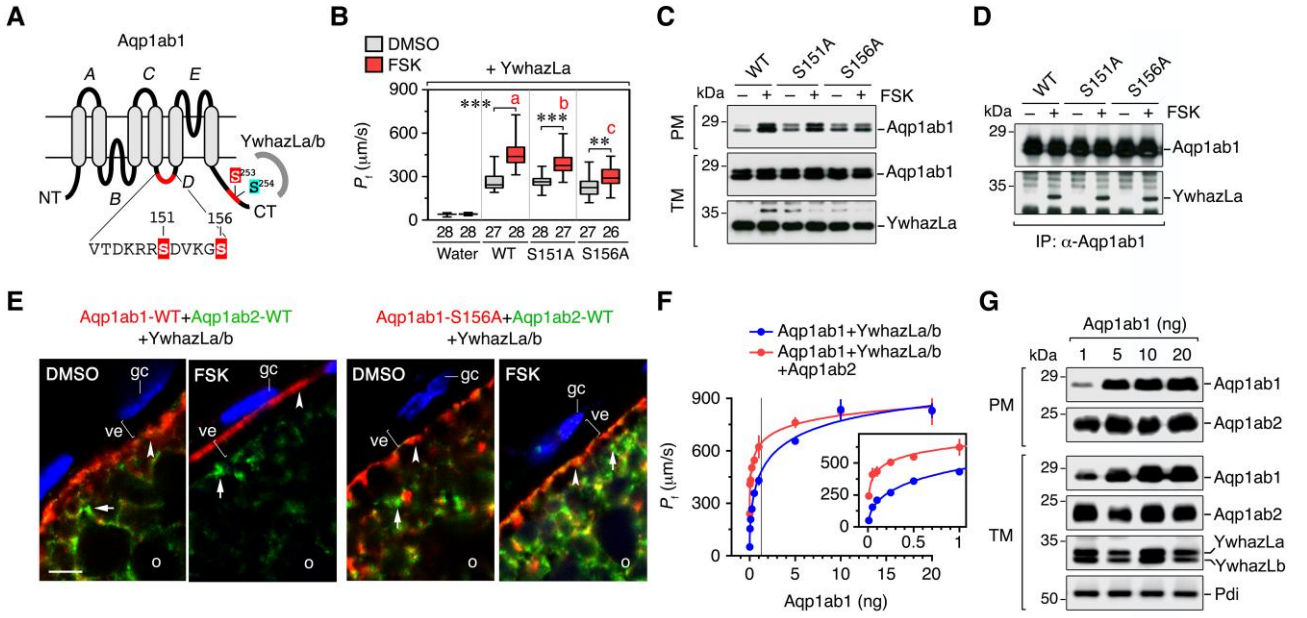

Fig. 6. Seabream Aqp1ab1 trafficking is regulated by dual phosphorylation of the cytoplasmic loop D and C-terminus of the channel. (*A*) Schematic representation of the SaAqp1ab1 monomer showing the C-terminus regulatory sites for YwhazLa or -zLb binding (S^{253}) and p38 MAPK phosphorylation (S^{254}), and the amino acid sequence of loop D with the two predicted PKA phosphorylation sites (S^{151} and S^{156}). (*B*) P_f of *X. laevis* oocytes injected with water or expressing SaAqp1ab1-WT or mutant channels in loop D (S151*A* and S156*A*), and treated with DMSO (control) or FSK. All oocytes were co-injected with YwhazLa-HA. Data are presented as box and whisker plots with the number of oocytes in each group indicated below the plot. For each construct, data were analyzed by the unpaired Student's *t*-test (**$P < 0.01$: ***$P < 0.001$; as indicated in brackets). Data from oocytes exposed to FSK were separately analyzed by one-way ANOVA ($P < 0.05$; different letters in red color indicate significant differences). (*C* and *D*) Immunoblot of Aqp1ab1 and YwhazLa in protein extracts of TM and PM from oocytes treated as in A (*C*), and of Aqp1ab1 co-immunoprecipitates (*D*). (*E*) Double immunostaining of Aqp1ab1 (red) and Aqp1ab2 (green) in *X. laevis* follicle-enclosed oocytes expressing WT Aqp1ab1 (red) or Aqp1ab1-S156*A* (red), and Aqp1ab2 (green), YwhazLa and -zLb, and treated with DMSO or FSK. gc, granulosa cells; ve, vitelline envelope; o, oocyte. Scale bar, 5 µm. (*F*) P_f of oocytes expressing increasing amounts of Aqp1ab1 cRNA (0.05–20 ng) and fixed amounts of YwhazLa and -zLb (15 ng), in the presence or absence of Aqp1ab2 (20 ng) expression, and treated with FSK. The insert shows the P_f of oocytes injected from 0.05 up to 1 ng Aqp1a1 cRNA. (*G*) Immunoblot of Aqp1ab1, -1ab2, YwhazLa, and -zLb in TM and PM protein extracts from oocytes treated as in F. In C, D, and G, molecular mass markers are on the left.

Aqp1ab1 and -1ab2 to the distal and proximal regions of the oocyte microvilli, respectively (fig. 5*H* and supplementary fig. S22, Supplementary Material online), as observed in the in vivo hydrating oocytes, and increased water permeability with respect to DMSO-treated (control) follicles (fig. 5*I*). Co-immunoprecipitation confirmed that in control follicles Aqp1ab1 was already phosphorylated and bound to both YwhazLa and -zLb (fig. 5*J*), without the channel trafficking to the distal region of the oocyte microvilli. However, when such distal membrane trafficking is activated by FSK, Aqp1ab1 becomes more phosphorylated, while maintaining the interaction with YwhazLa and -zLb (fig. 5*J*). Phosphorylation of Aqp1ab2 was also increased after FSK stimulation, but in this case, the YwhazLb interaction was only detected in the presence of FSK, when the channel is translocated to the basal region of oocyte microvilli (fig. 5*K*).

Dual Phosphorylation Generates a Two-Step Regulation of Aqp1ab1 Trafficking to Avoid Competitive PM Occupancy During Oocyte Hydration

The previous data suggested that Aqp1ab1 and -1ab2 phosphorylation in seabream oocytes mediates the YwhazL interaction to facilitate channel trafficking to the PM. However, the binding of Aqp1ab1 to YwhazL proteins apparently does not induce channel shuttling to the distal region of the oocyte microvilli. Rather, this mechanism appears to be associated with an additional phosphorylation of Aqp1ab1, indicating that a second PKA-mediated phosphorylation event of Aqp1ab1 may have evolved in pelagophil euacanthomorph teleosts. To investigate this hypothesis, we re-examined the role of the two predicted PKA phosphorylation sites in loop D of seabream Aqp1ab1 (Ser^{151} and Ser^{156}) in channel trafficking (fig. 6*A*), either of which is conserved in >95% of marine euacanthomorphs that spawn pelagic eggs such as Atlantic halibut (supplementary fig. S10*F*, Supplementary Material online). Experiments using *X. laevis* oocytes showed that the increment of the P_f of FSK-treated oocytes co-expressing SaAqp1ab1-S151A or -S156A plus YwhazLa was reduced when compared to oocytes injected with wild-type (WT) SaAqp1ab1 and YwhazLa, the reduction being more prominent in the S156A mutant-expressing oocytes (fig. 6*B*). Co-immunoprecipitation and immunoblotting corroborated that none of the mutants prevented the YwhazLa interaction (fig. 6*C* and *D*), but the relative amount of the S156A mutant in the oocyte PM was lower than that of

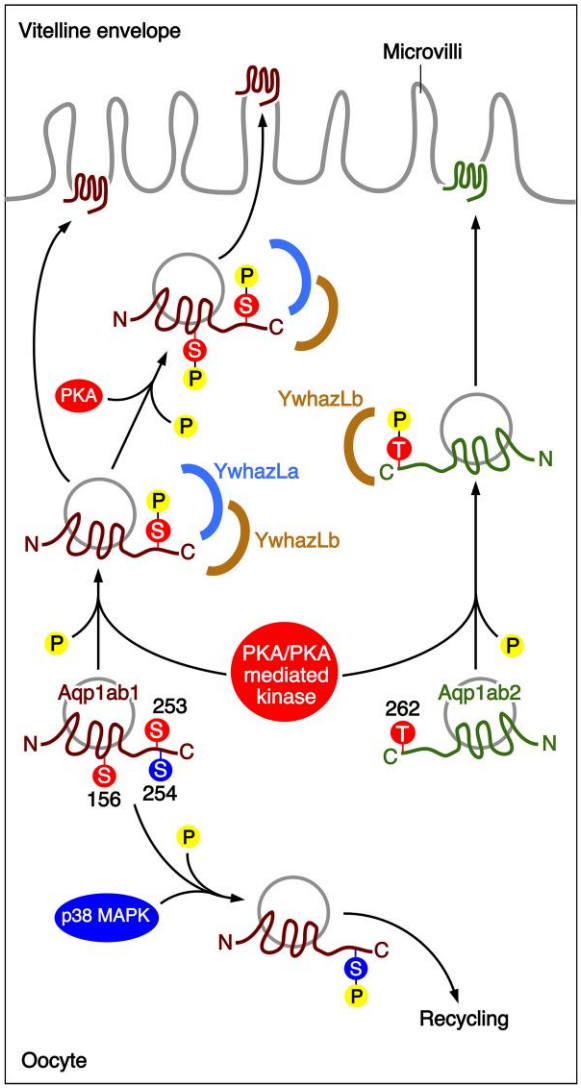

Fig. 7. Proposed model for the regulatory pathways controlling Aqp1ab1 and -1ab2 intracellular trafficking during oocyte hydration in the marine euacanthomorph teleost gilthead seabream. During vitellogenesis, Aqp1ab1 is phosphorylated at Ser^{253} by PKA (or by another kinase activated by PKA) to bind YwhazLa and -zLb, and the complex is transported to the oocyte cortical region, where it is retained just below the oocyte PM. At this stage, Aqp1ab2 is not bound to YwhazLb and remains in the cytoplasm. When meiosis resumption and yolk hydrolysis are activated in oocytes by hormonal signals, the Aqp1ab1 channel complexed with YwhazLa or -zLb is phosphorylated again by PKA at Ser^{156} in loop D, which further shuttles Aqp1ab1 to the most distal region of the oocyte microvilli. At this time, Aqp1ab2 is also phosphorylated by PKA at Thr^{262}, which drives the YwhazLb interaction and the trafficking of the channel to the proximal region of the oocyte microvilli. This model may explain how marine euacanthomorph teleosts that retain a complete TSA1C evolved subfunctionalized mechanisms involving protein kinases and specific YwhazL proteins for the trafficking regulation of the downstream Aqp1ab-type paralogs, such that competitive PM spatial occupancy is avoided and the bulk water flow is augmented during oocyte hydration.

the WT (fig. 6C). Immunostaining of intact *X. laevis* ovarian follicles expressing YwhazL proteins and SaAqp1ab2, together with WT SaAqp1ab1 or the S156A mutant, and exposed to FSK, revealed that WT SaAqp1ab1 was trafficked to the most distal region of the oocyte microvilli traversing the vitelline envelope, whereas the S156A mutant remained retained in the microvillar proximal region (fig. 6E). In contrast, SaAqp1ab2 was accumulated in the proximal region of the microvilli in response to FSK, regardless of the co-expression with the WT SaAqp1ab1 or the S156A mutant (fig. 6E). These data therefore suggest that when Aqp1ab1 is bound to YwhazLa or -zLb, a second PKA-mediated phosphorylation of a loop D Ser is the mechanism by which the channel is shuttled to the distal region of the oocyte microvilli, thus avoiding competitive PM spatial occupancy with Aqp1ab2 during oocyte hydration.

To finally investigate the physiological relevance of non-competitive membrane space occupancy of Aqp1ab channels during oocyte hydration, *X. laevis* oocytes were injected with increasing amounts of SaAqp1ab1 cRNA and fixed amounts of YwhazLa and -zLb, in the presence or absence of a constant dose of SaAqp1ab2, followed by P_f determination and immunoblot analysis after FSK treatment. At low doses of SaAqp1ab1 cRNA, the P_f of oocytes correlated well with the protein expression levels and the accumulation of the channel in the oocyte PM, whereas at high doses of SaAqp1ab1 the P_f and the expression levels reached a plateau (fig. 6F and G), possibly indicating the saturation of the oocyte translation machinery. However, co-expression of SaAqp1ab2 with low doses of SaAqp1ab1 resulted in an increased oocyte P_f, which was no longer observed when high doses of SaAqp1ab1 were injected in the oocytes (fig. 6F). These data indicate that expression of Aqp1ab1 and -1ab2 in different regions of the oocyte PM augments the bulk rate of aquaporin-mediated water flow.

A Model for the Regulation of Aqp1ab1 and -1ab2 Intracellular Trafficking During Oocyte Hydration in Marine Euacanthomorph Teleosts

By integrating the functional data obtained in this study for the seabream, a new model for the molecular regulation of Aqp1ab1 and -1ab2 intracellular trafficking during oocyte hydration in marine euacanthomorph teleosts that retain both paralogs can be proposed (fig. 7). During vitellogenesis, Aqp1ab1 is phosphorylated at Ser^{253} by PKA to bind YwhazLa and -zLb, and the complex is transported to the oocyte cortical region, where it is retained just below the oocyte PM. At this stage, Aqp1ab2 is not bound to YwhazLb and remains in the cytoplasm. When oocyte meiosis resumption and yolk hydrolysis are activated by hormonal signals (Fabra et al. 2006), the Aqp1ab1 channel complexed with YwhazLa or -zLb is further phosphorylated by PKA at Ser^{156} in loop D, which further shuttles Aqp1ab1 to the most distal region of the oocyte microvilli. Activation of PKA also phosphorylates Thr^{262} in Aqp1ab2, which drives the YwhazLb interaction and the trafficking of the channel to the proximal region of the oocyte microvilli. After hydration, Aqp1ab1 is probably phosphorylated by p38 MAPK at Ser^{254}, which prevents the YwhazL interaction needed for continued trafficking, while also likely decreasing Aqp1ab1

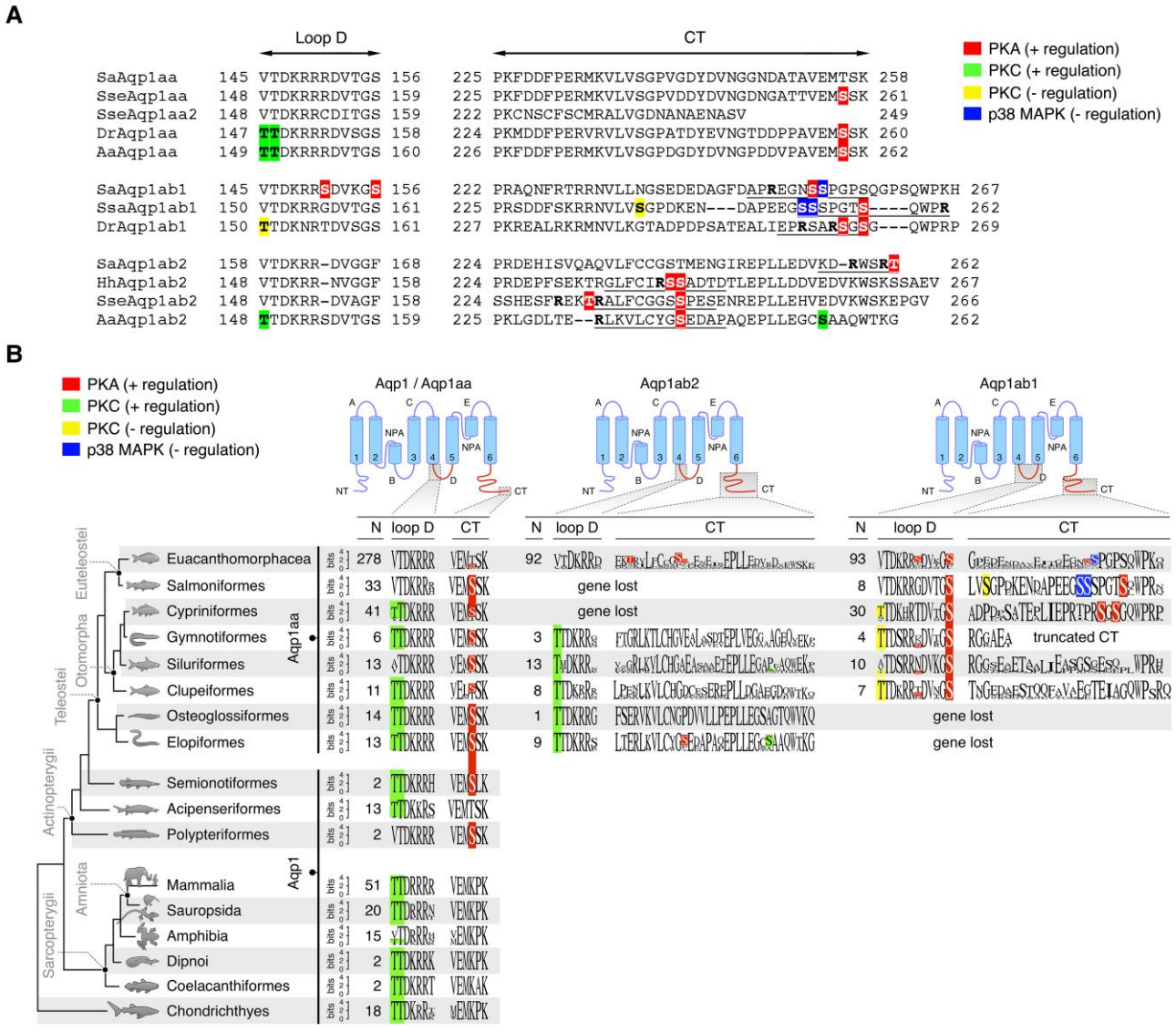

Fig. 8. Evolution of phosphorylation sites regulating the membrane trafficking of vertebrate aquaporin-1 channels. (*A*) Aligned amino acid sequences of loop D and the carboxyl termini (CT) of Aqp1aa, -1ab1, and -1ab2 paralogs from distantly related teleosts showing the specific residues involved in PKA, PKC, and p38 MAPK regulation of channel trafficking as experimentally determined in this study using *X. laevis* oocytes. The YwhazLa and -zLb binding regions in Aqp1ab1 and -1ab2, respectively, are underlined. (*B*) Cartoon aquaporin structures indicating the intracellular domains for the consensus sequences for loop D and the CT which are scaled according to residue prevalence and illustrate the conservation or substitution of PKA, PKC, and p38 MAPK phosphorylation sites in different vertebrate groups. The number of taxa (*N*) used to calculate each consensus sequence is given.

half-life so that the channel is directed into the degradation pathway (Moeller et al. 2016). Simultaneously, the interaction of Aqp1ab2 with YwhazLb is also terminated by a yet unknown mechanism that dissociates YwhazLb binding, or due to a decreased synthesis of YwhazLb in the oocyte, such that this paralog also ceases its trafficking to the PM. The model shows how marine euacanthomorph teleosts that retain a complete TSA1C evolved subfunctionalized mechanisms involving protein kinases and specific YwhazL proteins for the regulation of the trafficking of the downstream Aqp1ab-type paralogs such that competitive PM spatial occupancy is avoided and the bulk water flow is augmented during oocyte hydration.

Discussion

The origin of the extraordinary diversity of modern marine euacanthomorph teleosts has yet to be fully explained. Since the earliest teleosts are estimated to have arisen toward the end of the Paleozoic Era ~300 Ma in the aftermath of an R3 WGD (Hurley et al. 2007; Amores et al. 2011; Near et al. 2012; Hughes et al. 2018), it has been suggested that the additional gene repertoires and their subsequent neo-/subfunctionalization could have provided the genetic material for the radiative success (Hoegg et al. 2004; Postlethwait et al. 2004). However, the large chronological gap (~245 million years) between the R3 event and the explosive radiation of the Euacanthomorphacea in

marine environments ~55 Ma, together with the rediploidization of the genomes (Lien et al. 2016; Van de Peer et al. 2017) are considered problematic for single causal events such as R3 (Santini et al. 2009). Indeed, a similar uncoupling between WGD events and adaptation potential has been noted for plants (Schranz et al. 2012). In this work, we uncover an ancient TSA1C together with novel molecular regulatory mechanisms that co-evolved to provide the majority of marine euacanthomorph embryos with the water of life when no osmoregulatory systems exist. The process of oocyte hydration, which occurs during the final meiotic maturation stages of oogenesis, is so efficient that the spawned eggs typically achieve water contents of >90% so that they float pelagically for dispersal in the oceanic currents. In contrast to previous studies (Fabra et al. 2005, 2006; Kagawa et al. 2009; Zapater et al 2011), we show here that the mechanism of oocyte hydration involves in fact two tandemly duplicated *aqp1ab*-type genes that are selectively retained in species that spawn pelagic eggs. The phylogenetic and synteny analyses of piscine *aqp1*-type genes revealed that two of the three main lineages of extant teleosts (Elopomorpha and Osteoglossomorpha) still encode the R3 ohnologs (*aqp1aa* and *aqp1b*), and that the teleost-specific *aqp1ab*-type genes only duplicated downstream of the *aqp1aa* paralog to form the TSA1C. Since we did not find traces of the *aqp1ab*-type genes in the genomes of the preteleost actinopterygian lineages, yet observe that the osteoglossomorph teleosts still retain pseudogene remnants of *aqp1ab1* and *-1ab2*, the tandem duplication event likely occurred soon after R3 and was thus ancient and specific for teleosts.

The consequences of gene duplication have been widely recognized, with stochastic silencing and loss occurring as the most prevalent outcome within a few million years (Lynch and Conery 2000). This type of outcome fits the evolution of the *aqp1b* ohnologs, which are seemingly extinct in all clupeocephalan teleosts. Conversely, gene preservation is associated with the acquisition of novel (neo-) or split (sub-) functions (Force et al. 1999). In the present context, we find that all three processes have continued to impact the trajectories of *aqp1ab*-type genes throughout ~300 million years of teleost evolution. The data show that many lineages have lost or only retain fragmented pseudogenes of both paralogs, while others have lost either the *aqp1ab1* or *-1ab2* gene, yet many species still retain both of the tandem duplicates. An overwhelming majority (95%) of species that spawn pelagic eggs in marine environments retain at least one of the duplicates, with a third of the species still harboring complete copies of both paralogs. Conversely, much higher levels of gene loss are seen in species that spawn benthic eggs (43%) or incubate their eggs internally (91%). In marine benthic eggs, oocytes hydrate to a significantly lower degree than pelagic eggs, reaching water contents of 68–82% of egg wet mass (Finn et al., 2002a, 2002b), while the eggs of seahorses and pipefishes, which are incubated in the male brood pouch that remains hyposmotic to SW (Ripley 2009), do not hydrate (Finn, unpublished data).

Although some species of FW teleosts also retain the TSA1C, with *aqp1ab*-type gene expression occurring in extraovarian tissues (Cerdà and Finn 2010; Engelund and Madsen 2014; Cerdà et al. 2017), our present and previous data (Tingaud-Sequeira et al. 2008; Zapater et al. 2011) show that *aqp1ab1* and *-1ab2* transcript enrichment within the ovaries of marine pelagophil species are orders of magnitude higher than in the somatic tissues and that both channels are localized in the same PM of hydrating oocytes. Such a colocalization of closely related water-selective channels is unexpected, since it may imply redundant membrane space occupancy. This observation, together with the absence of membrane trafficking when Aqp1ab2 was heterologously expressed in amphibian oocytes, prompted us to investigate the intracellular trafficking regulation of the TSA1C channels.

By comparing the subdomains of the teleost TSA1C channels to the Aqp1 orthologs of nonteleost vertebrates, it became evident that the regulatory sites in the Aqp1 and Aqp1aa orthologs have remained relatively fixed through time, while those of the Aqp1ab1 and −1ab2 channels have selectively changed during teleost evolution (fig. 8). For example, PKC positively regulates the membrane trafficking of the Aqp1/Aqp1aa orthologs through phosphorylation of a conserved Thr in loop D in most vertebrate groups except some amphibians, Polypteriformes, Siluriformes, and Euteleostei, which encode a Val or Ala. The Thr/Val substitution in Euteleostei resulted in the loss of the positive PKC-mediated regulation and the emergence of a negative PKC-mediated regulation. Further, in contrast to Chondrichthyes and Sarcopterygii, many actinopterygian fishes evolved a C-terminal Ser for positive regulation via PKA-mediated phosphorylation. Nevertheless, even in euacanthomorph species in which the Aqp1aa C-terminal PKA site is conserved, as in Senegalese sole, an alternative negative PKC-mediated regulation still exists, while the positive PKA-mediated regulation of the older lineages is also maintained.

In contrast to the Aqp1/Aqp1aa, the two Aqp1ab-type channels evolved PKA, PKC, and p38 MAPK regulatory sites that are both dependent and independent of the teleost-specific YwhazL binding proteins (fig. 8). The identification of the novel YwhazLa and -zLb paralogs in the present study extend recent findings reporting that ostariophysan teleosts encode duplicated *ywhaz* genes of the mammalian *YWHAZ* ortholog (Zhang et al. 2021). In this context, however, we note that the *ywhazLa* gene synteny is only conserved between Otophysi and osteoglossomorph teleosts, while the *ywhazLb* gene is only syntenic within the Ostariophysi (e.g., zebrafish and catfishes). The novel *ywhazLa* and *-zLb* genes identified here cluster within the vertebrate *ywhaz* clade, but are polyphyletic and are not syntenic between euacanthomorph and the more basal teleost lineages. Their neofunctionalization can be inferred from the longer branch lengths, and the mutagenesis experiments show their specific functional requirement for PM trafficking of the Aqp1ab-type channels. For example, in the basal cohort of elopomorph teleosts, such as the

European eel, which spawn pelagic eggs and only retain the Aqp1ab2 paralog, PKA-mediated positive regulation of membrane trafficking is dependent on C-terminal YwhazLa binding and two YwhazLa-independent PKC-regulated sites in loop D and the C-terminus, respectively (fig. 8). In modern lineages of euacanthomorph species that retain both the Aqp1ab2 and -1ab1 paralogs, the PKC-mediated regulation of Aqp1ab2 is lost, and membrane trafficking became dependent on PKA-mediated phosphorylation of the same C-terminal Ser residues as in the elopomorph teleosts, but dependent on YwhazLb rather than YwhazLa binding.

A more intricate regulation of membrane trafficking evolved in the teleost Aqp1ab1 channels (fig. 8). Amongst cyprinid species, such as zebrafish, PKA-mediated phosphorylation of different Ser residues in the C-terminus positively regulates membrane trafficking, on both YwhaLa-dependent and independent manner, while PKC-mediated phosphorylation in loop D recycles the channel. In salmonids, such as the Atlantic salmon, only the positive PKA-mediated regulation in the C-terminus that is dependent on YwhazLa binding is maintained, while new C-terminal recycling sites emerge that are regulated by PKC (outside of the YwhazLa binding domain) and p38 MAPK (within the YwhazLa binding site). The p38 MAPK negative regulatory site in the YwhazLa binding region is maintained in euacanthomorph teleosts, such as seabream, together with a positive PKA-mediated YwhazLa-dependent site. However, two additional positive PKA-mediated regulation sites appear in loop D of Aqp1ab1 that depend on the binding of the channel to YwhazLa. It is this latter two-step regulation that generates a membrane trafficking shunt of Aqp1ab1 to the distal region of the microvilli, and thus the avoidance of competitive occupancy of the same membrane space as the Aqp1ab2 channel. In contrast, Aqp1ab2 is dependent on YwhazLb binding, lacks the loop D regulatory step, and thus remains in the proximal region of the PM. Our ex vivo experimental data also show that the Aqp1ab1 membrane shunt can be recapitulated in the surrogate *X. laevis* oocytes co-expressing Aqp1ab1, -1ab2, and the YwhaL binding proteins, resulting in an increase in the bulk rate of water transport.

The combined findings thus shed new light on the molecular adaptations facilitating the success of teleost eggs in the oceans. To survive in the harsh hyperosmotic saline environment, teleosts evolved adaptive solutions that provide their hyposmotic marine embryos with the water of life prior to the development of homeosmotic regulatory systems. The process involved the selective retention of duplicated *aqp1ab*-type water channel genes that are tandemly arranged in an ancient ternary cluster, the TSA1C. Each channel co-evolved with specific YwhazL regulatory proteins and PKA-, PKC-, and p38 MAPK-mediated phosphorylation pathways to regulate the hydration of the oocytes. The most intricate solutions evolved in the highly diverse marine euacanthomorph teleosts that retain both of the Aqp1ab1 and -1ab2 channels. In such species, an innovative membrane shunt evolved that avoids competitive space occupancy in the oocyte PM and an increase in the rate of bulk water influx during hydration. The hydration process is terminated though the evolution of p38 MAPK-mediated phosphorylation sites in the YwhazLa binding region of Aqp1ab1, which dissociates the interaction with YwhazLa, and through a different mechanism also resulting in the release of the YwhazLb from Aqp1ab2. Both mechanisms consequently induce the recycling of the two Aqp1ab-type channels from the PM, so that >90% of the egg water content remains locked within the yolk cell due to the reduction in the oocyte permeability. When fertilized, the water-endowed eggs with a recombined allelic potential have a lower specific gravity than the surrounding SW and they thus float as passive pelagic passengers in the oceanic currents, which geodisperse them to new horizons.

Materials and Methods

Animals and Reagents

Fish were obtained from different aquaculture stations in Spain and Norway, whereas adult *X. laevis* were purchased from the Centre de Ressources Biologiques Xénopes (University of Rennes, France). Details relating to the care and use of fish and frogs are described in (supplementary text S1, Supplementary Material online). All reagents were purchased from Merck unless indicated otherwise. The commercial and custom-made antibodies employed are described in (supplementary table S3, Supplementary Material online).

Phylogenetic, Syntenic, and Structural Analyses

Sequences were assembled from open-source databases, aligned, and converted to codons before analysis via Bayesian inference, with in silico sequence analyses performed as described in (supplementary text S1, Supplementary Material online). A list of aquaporin type, spawning habitat, and egg type according to fishbase (https://www.fishbase.se/) is provided in (supplementary table S1, Supplementary Material online). The syntenic analyses of the aquaporin genes were conducted via tblastn searches of whole genome sequencing databases. Scaled sequence logos illustrating the relative conservation of residues in the aquaporin loop D and C-terminus-subdomains were generated with Geneious v9.1.8 (Biomatters Ltd, New Zealand).

Transcriptome Shotgun Sequencing

Illumina RNA-seq library construction and HiSeq2500 sequencing were carried out to sequence the transccriptome of Atlantic halibut and *X. laevis* postvitellogenic ovarian follicles. The complete methods for the novo assembly of the transcriptomes and the identification of YWHA orthologs are described in (supplementary text S1, Supplementary Material online).

Expression Constructs and Site-Directed Mutagenesis

The teleost aquaporin and YwhazL cDNAs employed in this study, and their GenBank accession numbers, are indicated in (supplementary text S1, Supplementary Material online). The cDNAs were subcloned into the pT7Ts (Deen et al. 1994) or pcDNA3 (Invitrogen) expression vectors, and in most cases fused with an HA or flag epitope tag at the N- or C-terminus of the encoded proteins by using polymerase chain reaction (PCR). Mutations into the loop D or C-terminal amino acid sequence of aquaporins were introduced by using the QuikChange lightning kit (Agilent Technologies; 210518) following the manufacturer's instructions. Substitution of the Aqp1ab1 or -1ab2 complete C-terminus for that of Aqp1aa was carried out by PCR as previously described (Tingaud-Sequeira et al. 2008). All constructs were verified by DNA Sanger sequencing to confirm that only the desired chimeras or mutations were produced.

Expression *in X. laevis* Oocytes and Swelling Assays

The cRNAs corresponding to the different constructs were synthesized in vitro with T7 RNA polymerase from *Xba*I-digested pT7Ts vector containing the cDNAs. The isolation and microinjection of oocytes (0.5–15 ng of cRNA depending on the construct), as well as the swelling assays, were carried out as previously described (Deen et al. 1994; Chauvigné et al. 2011). The effect of PKC or PKA activation on the oocyte P_f was tested by preincubating the oocytes with 100 nM PMA for 30 min, or with 100 µM IBMX for 1 h and subsequently with 100 µM FSK for 30 min, before determination of oocyte swelling or protein extraction. The effect of p38 MAPK activation was tested using 100 µM anisomycin (ANS). Control oocytes were treated with 0.1% of the drug vehicle dimethyl sulfoxide (DMSO).

In Vitro Incubation of Seabream Ovarian Follicles and Water Uptake Assays

Ovarian follicles at a different developmental stage were collected from naturally spawning seabream females and the P_f of follicles at each stage was determined under hypertonic conditions as previously described (Fabra et al. 2006; Zapater et al. 2011). For in vitro incubations, groups of ten postvitellogenic follicles were placed in 75% Leivovitz L-15 culture medium with L-glutamine and treated with 100 µM IBMX and 100 µM FSK for 1 h at 18 °C, or with 0.1% DMSO (controls). After incubation, follicles were fixed for immunofluorescence microscopy or used for water uptake assays. For this, follicles were transferred to 200 µl ultrapure water containing 10 µCi [^{3}H] water (1 mCi/ml) (American Radiolabeled Chemicals Inc., ART 0194A) for 20 min at room temperature. Follicles were washed twice in distilled water, dissolved in 400 µl of 10% sodium dodecyl sulfate (SDS) for 1 h, mixed with 4 ml of liquid scintillation cocktail (Perkin Elmer LLC Ultima Gold; LLC6013326), and counted using a Beckman Coulter scintillation counter. Some follicles were exposed to [^{3}H] water for 1 min and immediately washed in water for the subtraction of the background signal from the externally bound solute.

Protein Extraction and Immunoblotting

The total membrane (TM) and PM fractions of *X. laevis* oocytes ($n = 10$) and seabream ovarian follicles ($n = 50$) were isolated as described previously (Kamsteeg and Deen 2001). For the seabream follicles, the final pellet was resuspended in 1 × Laemmli sample buffer supplemented with 1 mM NaF, 1 mM Na_3VO_4, and protease inhibitors. In some experiments, whole protein extracts from seabream follicles were obtained by homogenization in 500 µl of radioimmunoprecipitation assay buffer (150 mM NaCl, 50 mM Tris pH 8.0, 1.0% Triton X-100, 0.5% sodium deoxycholate, 0.1% SDS, supplemented with 1 mM NaF, 1 mM Na_3VO_4, protease inhibitors, and 80 U benzonase) using a glass douncer, and further incubation on ice for 15 min. The samples were then centrifuged at 14,000 × *g* at 4 °C for 1 min, and the supernatant was mixed with 2 × Laemmli sample buffer and heated at 95 °C for 10 min. In some cases, lysates were digested with calf intestine alkaline phosphatase (New England Biolabs Inc.; M0525) for 1 h at 37 °C before Laemmli sample buffer addition. Immunoblotting was subsequently carried out as previously described (Zapater et al. 2011).

Co-Immunoprecipitation

X. laevis oocytes and seabream follicles were homogenized in the lysis buffer from the Pierce Crosslink Magnetic immunoprecipitated products (IP)/Co-IP Kit (Pierce; 88805) with a bouncer on ice, and centrifuged at 14,000 × *g* for 1 min. An aliquot (10%) of the protein extract was collected as the input of the IP and mixed with 2 × Laemmli sample buffer, whereas the remaining extract was incubated overnight at 4 °C under constant agitation with magnetic beads previously coated with anti-HA, anti-SaAqp1ab1 or anti-SaAqp1ab2 antibodies. For rabbit primary antibodies, the IP was carried out using the kit indicated above, and final eluted proteins in 50 µl of elution buffer were mixed with 4 × Laemmli sample buffer supplemented with protease and phosphatase inhibitors. For chicken antibodies, the IP was performed using Dynabeads M-280 Tosylactivated (Invitrogen; 14203) following the manufacturer's instructions. The input and immunoprecipitated samples were immunoblotted as indicated above.

Immunofluorescence Microscopy and Quantification

Samples were processed and immunostained as previously described (Chauvigné et al. 2018). Control sections were incubated without primary antibodies (when using commercial antibodies) or with antibodies preincubated with the corresponding peptides used for immunization (for custom-made antibodies). Double immunostaining using rabbit antibodies against seabream Aqp1ab1 and either YwhaLa/b or -zLb was performed by staining first for YwhaLa/b or -zLb as described above using an antirabbit

Cy3-coupled secondary antibody. After fixing with 4% paraformaldehyde (PFA) for 1 h, slides were incubated with the Aqp1ab1 antibody previously labeled with Zenon Rabbit IgG Alexa Fluor 488 Labeling Kit (Invitrogen, Z25302) following manufacturer instructions. After 1 h, sections were washed and fixed again with PFA for 15 min, incubated with 4′,6-diamidino-2-phenylindole (DAPI; 1:10,000), and mounted with Fluoromount aqueous mounting medium (F4680). Immunofluorescence was observed and documented with a Zeiss Axio Imager Z1/Apotome fluorescent microscope (Carl Zeiss Corp.). Changes in Aqp1ab1, -1ab2, YwhazLa/b, and -zLb abundance in the PM of seabream oocytes were evaluated by measuring the fluorescence intensity of the microvilli crossing the vitelline envelope with respect to the total fluorescence (PM plus cytoplasm) using the ImageJ software v.1.52o (https://imagej.nih.gov/ij/). For all treatments or developmental stages, the images were acquired with the same fluorescence exposure and similar orientation, so that the area of the PM and cytoplasm was equivalent.

Statistics

Comparisons between two independent groups were made by the two-tailed unpaired Student's *t*-test. The statistical significance among multiple groups were analyzed by one-way ANOVA, followed by Tukey's multiple comparison test, or by the nonparametric Kruskal–Wallis test and further Dunn's test for nonparametric post hoc comparisons. Percentages were square root transformed previous analyses. Differences between proportions were tested via the critical *z*-value approach. Statistical analyses were carried out using GraphPad Prism v9.1.2 (226) (GraphPad Software). In all cases, statistical significance was defined as $P < 0.05$ (*), $P < 0.01$ (**), or $P < 0.001$ (***).

Supplementary Material

Supplementary data are available at *Molecular Biology and Evolution* online.

Acknowledgments

We thank Michael Dondrup (University of Bergen, Norway) and Per Gunnar Fjelldal (Institute of Marine Research, Norway) for assistance in bioinformatic analysis and collection of biological samples from Atlantic salmon, respectively. This work was supported by the Spanish Ministry of Science and Innovation (MCIN/AEI/10.13039/501100011033), the European Regional Development Fund (ERDF) "A way of making Europe" (European Union), Grant no. AGL2016-76802-R (to J.C.), and the Norwegian Research Council (RCN) Grant no. 294768/E40 (to R.N.F). F.C. and A.F. were supported, respectively, by the "Ramon y Cajal" programe (RYC-2015-17103) and a predoctoral (BES-2014-068745) contract from Spanish MCIN. R.N.F. was also supported by the University of Bergen (Norway).

Author Contributions

J.C. and R.N.F. designed the study. B.N. and L.B. provided biological samples and genomic sequences. R.N.F. and J.C. carried out the phylogenetic and in silico analyses. A.F., F.C., and M.C. performed wet laboratory experiments and collected data. A.V., R.G., and R.N.F. carried out RNA-seq analysis. A.F., F.C., R.N.F., and J.C. interpreted the results. J.C. acquired the funding and supervised the work. J.C. and R.N.F. wrote the manuscript. All authors approved the final version of the manuscript.

Conflict of Interest: The authors declare that they have no competing interests.

Data Availability

Data underlying this article are available in the article and in its online supplementary material.

References

Agre P, Sasaki S, Chrispeels MJ. 1993. Aquaporins: a family of water channel proteins. *Am J Physiol*. **265:**F461.

Ahlstrom EH, Moser HG. 1981. Systematics and development of early life history stages of marine fishes: achievements during the past century, present status and suggestions for the future. *Rapp P-v Réun Cons int Explor Mer*. **178:**541–546.

Albalat R, Cañestro C. 2016. Evolution by gene loss. *Nat Rev Genet*. **17:**379–391.

Amores A, Catchen J, Ferrara A, Fontenot Q, Postlethwait JH. 2011. Genome evolution and meiotic maps by massively parallel DNA sequencing: spotted gar, an outgroup for the teleost genome duplication. *Genetics* **188:**799–808.

Berthelot C, Brunet F, Chalopin M, Juanchich A, Bernard M, Noel B, Bento P, Da Silva C, Labadie K, Alberti A, *et al*. 2014. The rainbow trout genome provides novel insights into evolution after whole-genome duplication in vertebrates. *Nat Commun*. **5:**3657.

Cerdà J, Chauvigné F, Finn RN. 2017. The physiological role and regulation of aquaporins in teleost germ cells. In: Yang B, editor. *Advances in experimental medicine and biology. Vol. 969. Aquaporins*. Dordrecht: Springer. p. 149–171.

Cerdà J, Fabra M, Raldúa D. 2007. Physiological and molecular basis of fish oocyte hydration. In: Babin P, Cerdà J, Lubzens E, editors. *The fish oocyte: from basic studies to biotechnological applications*. Dordrecht: Springer. p. 349–396.

Cerdà J, Finn RN. 2010. Piscine aquaporins: an overview of recent advances. *J Exp Zool*. **313A**:623–650.

Chauvigné F, Ferré A, Cerdà J. 2021. The *Xenopus* oocyte as an expression system for functional analyses of fish aquaporins. *Methods Mol Biol*. **2218**:11–28.

Chauvigné F, Lubzens E, Cerdà J. 2011. Design and characterization of genetically engineered zebrafish aquaporin-3 mutants highly permeable to the cryoprotectant ethylene glycol. *BMC Biotechnol*. **11:**34.

Chauvigné F, Parhi J, Ducat C, Ollé J, Finn RN, Cerdà J. 2018. The cellular localization and redistribution of multiple aquaporin paralogs in the spermatic duct epithelium of a maturing marine teleost. *J Anat*. **233:**177–192.

Chauvigné F, Yilmaz O, Ferré A, Fjelldal PG, Finn RN, Cerdà J. 2019. The vertebrate Aqp14 water channel is a neuropeptide-regulated polytransporter. *Comm Biol*. **2:**462.

Crow KD, Smith CD, Cheng JF, Wagner GP, Amemiya CT. 2012. An independent genome duplication inferred from Hox paralogs in the American paddlefish - a representative basal ray-finned fish and important comparative reference. *Genome Biol Evol*. **4:**937–953.

Deen PM, Verdijk MA, Knoers NV, Wieringa B, Monnens LA, van Os CH, van Oost BA. 1994. Requirement of human renal water channel aquaporin-2 for vasopressin-dependent concentration of urine. *Science* **264:**92–95.

Du K, Stöck M, Kneitz S, Klopp C, Woltering JM, Adolfi MC, Feron R, Prokopov D, Makunin A, Kichigin I, *et al.* 2020. The sterlet sturgeon genome sequence and the mechanisms of segmental rediploidization. *Nat Ecol Evol*. **4:**841–852.

Engelund MB, Madsen SS. 2014. Tubular localization and expressional dynamics of aquaporins in the kidney of seawater-challenged Atlantic salmon. *J Comp Physiol B*. **185:**207–223.

Fabra M, Raldúa D, Bozzo MG, Deen PM, Lubzens E, Cerdà J. 2006. Yolk proteolysis and aquaporin-1o play essential roles to regulate fish oocyte hydration during meiosis resumption. *Dev Biol*. **295:** 250–262.

Fabra M, Raldúa D, Power DM, Deen PM, Cerdà J. 2005. Marine fish egg hydration is aquaporin-mediated. *Science* **307:**545.

Finn RN. 2007. The maturational disassembly and differential proteolysis of paralogous vitellogenins in a marine pelagophil teleost: a conserved mechanism of oocyte hydration. *Biol Reprod*. **76:** 936–948.

Finn RN, Cerdà J. 2011. Aquaporin evolution in fishes. *Front Physiol*. **2:**44.

Finn RN, Chauvigné F, Hlidberg JB, Cutler CP, Cerdà J. 2014. The lineage-specific evolution of aquaporin gene clusters facilitated tetrapod terrestrial adaptation. *PLoS One* **9:**e113686.

Finn RN, Fyhn HJ. 2010. Requirement for amino acids in ontogeny of fish. *Aquacult Res*. **41:**684–716..

Finn RN, Fyhn HJ, Norberg B, Munholland J, Reith M. 2000. Oocyte hydration as a key feature in the adaptive evolution of teleost fishes to seawater. In: Norberg B, Kjesbu OS, Taranger GL, Anderson E, Stefansson SO, editors. *Proceedings of the 6th International Symposium on the Reproductive Physiology of Fish*. Bergen: Institute of Marine Research and the University of Bergen. p. 289–291.

Finn RN, Kristoffersen BA. 2007. Vertebrate vitellogenin gene duplication in relation to the "3R hypothesis": correlation to the pelagic egg and the oceanic radiation of teleosts. *PLoS One* **2:** e169.

Finn RN, Østby G, Norberg B, Fyhn HJ. 2002a. *In vivo* oocyte hydration in Atlantic halibut (*Hippoglossus hippoglossus*); proteolytic liberation of free amino acids, and ion transport are driving forces for osmotic water influx. *J Exp Biol*. **205:** 211–224.

Finn RN, Wamboldt M, Fyhn HJ. 2002b. Differential processing of yolk proteins during oocyte hydration in fishes (Labridae) that spawn benthic and pelagic eggs. *Mar Ecol Progr Series*. **237**: 217–226.

Force A, Lynch M, Pickett FB, Amores A, Yan YL, Postlethwait J. 1999. Preservation of duplicate genes by complementary, degenerative mutations. *Genetics* **151:**1531–1545.

Friedman M. 2010. Explosive morphological diversification of spiny-finned teleost fishes in the aftermath of the end-cretaceous extinction. *Proc R Soc B* **277:**1675–1683.

Fu H, Subramanian RR, Masters SC. 2000. 14-3-3 Proteins: structure, function, and regulation. *Annu Rev Pharmacol Toxicol*. **40:** 617–647.

Fyhn HJ, Finn RN, Reith M, Norberg B. 1999. Yolk protein hydrolysis and oocyte free amino acids as key features in the adaptive evolution of teleost fishes to seawater. *Sarsia* **84:**451–456.

Gasanov EV, Jedrychowska J, Kuznicki J, Korzh V. 2021. Evolutionary context can clarify gene names: teleosts as a case study. *BioEssays* **43:**e2000258.

Hoegg S, Brinkmann H, Taylor JS, Meyer A. 2004. Phylogenetic timing of the fish-specific genome duplication correlates with the diversification of teleost fish. *J Mol Evol*. **59:**109–203.

Hughes LC, Orti G, Huang Y, Sun Y, Baldwin CC, Thompson AW, Arcila D, Betancur-R R, Li C, Becker L, *et al.* 2018. Comprehensive phylogeny of ray-finned fishes (actinopterygii) based on transcriptomic and genomic data. *Proc Natl Acad Sci U S A*. **115:**6249–6254.

Hurley IA, Mueller RL, Dunn KA, Schmidt EJ, Friedman M, Ho RK, Prince VE, Yang Z, Thomas MG, Coates MI. 2007. A new time-scale for ray-finned fish evolution. *Proc R Soc B*. **274:**489–498.

Kagawa H, Horiuchi Y, Kasuga Y, Kishi T. 2009. Oocyte hydration in the Japanese eel (*Anguilla japonica*) during meiosis resumption and ovulation. *J Exp Zool*. **311A**:752–762.

Kagawa H, Kishi T, Gen K, Kazeto Y, Tosaka R, Matsubara H, Matsubara T, Sawaguchi S. 2011. Expression and localization of aquaporin 1b during oocyte development in the Japanese eel (Anguilla japonica). *Reprod Biol Endocrinol*. **9**:71.

Kamsteeg EJ, Deen PM. 2001. Detection of aquaporin-2 in the plasma membranes of oocytes: a novel isolation method with improved yield and purity. *Biochem Biophys Res Commun*. **282:**683–690.

Kendall AW, Ahlstrom EH, Moser HG. 1984. Early life history stages of fishes and their characters. In: Moser HG, editor. *Ontogeny and systematics of fishes*. Lawrence, KS: American Society of Ichthyologists and Herpetologists Special publ 1. p. 11–22.

Lien S, Koop BF, Sandve SR, Miller JR, Kent MP, Nome T, Hvidsten TR, Leong JS, Minkley DR, Zimin A, *et al.* 2016. The Atlantic salmon genome provides insights into rediploidization. *Nature* **533:** 200–205.

Lynch M, Conery JS. 2000. The evolutionary fate and consequences of duplicate genes. *Science* **290:**1151–1155.

MacQueen DJ, Johnston I. 2014. A well-constrained estimate for the timing of the salmonid whole genome duplication reveals major decoupling from species diversification. *Proc R Soc B Biol Sci*. **281:** 20132881.

Maissey JG. 1996. *Discovering fossil fishes*. New York: Westview Press.

Moeller HB, Slengerik-Hansen J, Aroankins T, Assentoft M, MacAulay N, Moestrup SK, Bhalla V, Fenton RA. 2016. Regulation of the water channel aquaporin-2 via 14-3-3θ and -ζ. *J Biol Chem*. **291:**2469–2484.

Near TJ, Eytan RI, Domburg A, Kristen KL, Moore JA, Davis MP, Wainwright PC, Friedman M, Smith WL. 2012. Resolution of ray-finned fish phylogeny and timing of diversification. *Proc Natl Acad Sci U S A*. **109:**13698–13703.

Nesverova V, Törnroth-Horsefield S. 2019. Phosphorylation-dependent regulation of mammalian aquaporins. *Cells* **8:**82.

Postlethwait J, Amores A, Cresko W, Singer A, Yan YL. 2004. Subfunction partitioning, the teleost radiation and the annotation of the human genome. *Trends Genet*. **20:**481–490.

Prado K, Cotelle V, Li G, Bellati J, Tang N, Tournaire-Roux C, Martinière A, Santoni V, Maurel C. 2019. Oscillating aquaporin phosphorylation and 14-3-3 proteins mediate the circadian regulation of leaf hydraulics. *Plant Cell* **31:**417–429.

Rajan S, Preisig-Müller R, Wischmeyer E, Nehring R, Hanley PJ, Renigunta V, Musset B, Schlichthörl G, Derst C, Karschin A, *et al.* 2002. Interaction with 14-3-3 proteins promotes functional expression of the potassium channels TASK-1 and TASK-3. *J Physiol*. **545:**13–26.

Ripley JL. 2009. Osmoregulatory role of the paternal brood pouch for two Sygnathus species. *Comp Biochem Physiol*. **154A**:98–104.

Santini F, Harmon LJ, Carnevale G, Alfaro ME. 2009. Did genome duplication drive the origin of teleosts? A comparative study of diversification in ray-finned fishes. *BMC Evol Biol*. **9:**194.

Schranz ME, Mohammadin S, Edger PP. 2012. Ancient whole genome duplications, novelty and diversification: the WGD radiation lag-time model. *Curr Opin Plant Biol*. **15:**147–153.

Shikano S, Coblitz B, Sun H, Li M. 2005. Genetic isolation of transport signals directing cell surface expression. *Nat Cell Biol*. **7:**985–992.

Sullivan CV, Yilmaz O. 2018. *Vitellogenesis and yolk proteins, fish. Encyclopedia of reproduction*. 2nd ed. Elsevier Inc. p. 1–11.

Tingaud-Sequeira A, Calusinska M, Finn RN, Chauvigné F, Lozano J, Cerdà J. 2010. The zebrafish genome encodes the largest vertebrate repertoire of functional aquaporins with dual paralogy and substrate specificities similar to mammals. *BMC Evol Biol*. **10**:38.

Tingaud-Sequeira A, Chauvigné F, Fabra M, Lozano J, Raldúa D, Cerdà J. 2008. Structural and functional divergence of two fish aquaporin-1 water channels following teleost-specific gene duplication. *BMC Evol Biol*. **8:**259.

Van de Peer Y, Mizrachi E, Marchal K. 2017. The evolutionary significance of polyploidy. *Nat Rev Genet*. **18:**411–424.

Xu P, Xu J, Liu G-J, Chen L, Zhou Z, Peng W, Jiang Y, Zhao Z, Jia Z, Sun Y, *et al*. 2019. The allotetraploid origin and asymmetrical genome evolution of the common carp *Cyprinus carpio*. *Nat Commun*. **10:**4625.

Yilmaz O, Ferré A, Nilsen F, Fjelldal PG, Cerdà J, Finn RN. 2020. Unravelling the complex duplication history of deuterostome glycerol transporters. *Cells* **9:**1663.

Zapater C, Chauvigné F, Norberg B, Finn RN, Cerdà J. 2011. Dual neofunctionalization of a rapidly evolving aquaporin-1 paralog resulted in constrained and relaxed traits controlling channel function during meiosis resumption in teleosts. *Mol Biol Evol*. **28:**3151–3169.

Zapater C, Chauvigné F, Tingaud-Sequeira A, Finn RN, Cerdà J. 2013. Primary oocyte transcriptional activation of *aqp1ab* by the nuclear progestin receptor determines the pelagic egg phenotype of marine teleosts. *Dev Biol*. **377:**345–362.

Zhang X, Yu P, Wen H, Qi X, Tian Y, Zhang K, Fu Q, Li Y, Li C. 2021. Genome-wide characterization of aquaporins (aqps) in *Lateolabrax maculatus*: evolution and expression patterns during freshwater acclimation. *Mar Biotechnol*. **23:**696–709.